

# Distributed Acoustic Sensing: A New Tool or a New Paradigm

K. V. Kislov<sup>a,\*</sup> and V. V. Gravirov<sup>b</sup>

<sup>a</sup> *Institute of Earthquake Prediction Theory and Mathematical Geophysics, Russian Academy of Sciences, Moscow, 117997 Russia*

<sup>b</sup> *Schmidt Institute of Physics of the Earth, Russian Academy of Sciences, Moscow, 123242 Russia*

\*e-mail: kvkislov@yandex.ru

Received February 4, 2022; revised February 28, 2022; accepted March 4, 2022

**Abstract**—Distributed acoustic sensing (DAS) is a technology that uses a fiber optic cable as a linear array of virtual seismic sensors. The article allows the reader to learn a little more about DAS data, mainly from the theoretical viewpoint, and correct some existing misconceptions; it gives an overview of the development of DAS and its modifications. The objective of this work is to discuss the advantages and prospects of distributed fiber optic sensors and the possibilities of expanding the boundaries of their practical applications and to clarify the problems and limitations faced by seismologists using DAS. Ways of overcoming the existing limitations are also described. The article identifies areas which need to be developed for wider dissemination of distributed measurements; it lists some commercialized applications and applications in which experiments will soon turn into routine geophysical measurements.

**Keywords:** distributed acoustic sensing (DAS), distributed vibration sensing (DVS), distributed strain sensing (DSS), optic fiber, Rayleigh scattering, Brillouin scattering, stimulated Brillouin scattering, optic time domain reflectometry, optic frequency domain reflectometry, Brillouin optic analysis systems

**DOI:** 10.3103/S0747923922050085

## INTRODUCTION

The terms fiber optic distributed acoustic sensing (DAS), distributed vibration sensing (DVS), and distributed strain sensing (DSS) refer to the technology of using an optic fiber as a linear array of seismic instruments (Lu et al., 2019; Fanta et al., 2021). It measures the tension/compression in the fiber optic cable. These measurements are based on natural light scattering processes in optic fibers. The systems based on Rayleigh scattering are most often used, since they give a high signal level (Lindsey and Martin, 2021). Mandelstam–Brillouin scattering is also used (Lopez Mercado et al., 2021). When a light pulse passes through a fiber, each of its sections, understood by us as a virtual seismic instrument, scatters part of the light. Backscattered light can be recorded at the beginning of the cable, with each segment of the recording corresponding to its own segment of the segment. If the backscattering in this segment changes in amplitude or phase during passage of the next pulse, then the fiber optic cable is affected in some way. Thus, an optic fiber is used both for information transmission and as a set of sensors.

In the literature devoted to this topic, especially in Internet resources, a lot of abbreviations are used, often without decoding. Table 1 contains a brief glossary of the most common terms. In the body of the article, we also use the generally accepted abbreviations from Table 1.

## BRIEF HISTORY

Light has been used to transmit information since ancient times (Figs. 1–3). With the advent of optic interferometry, it began to find application in measuring systems. The first application of interferometry was Newton’s rings (Fig. 4), which arise due to the gap between a studied part study and the test glass. Surface curvature deviation is expressed as the number of interference rings.

The largest steps that led to the creation of DAS technology were the inventions of the laser and fiber optics (Table 2) (*Volokonno-opticheskaya...*, 2000). Optic fibers are widely used in geophysics (Rajan, 2017; Ilinskiy et al., 2021; Bakulin et al., 2020; Gutscher et al., 2020; Matias et al., 2020; Luo et al., 2021; Yuan Q. et al., 2021). In addition to data transmission lines, Bragg grating sensors are used (Daley et al., 2013; Hong et al., 2016; Henniges et al., 2020; Liu S.P. et al., 2021), fiber optic gyroscopes (Kislov and Gravirov, 2021), fiber optic accelerometers and seismometers (Howe et al., 2019; Chang et al., 2020), fiber optic hydrophones (Ramakrishnan et al., 2013; Meng et al., 2021), interferometer systems (Marra et al., 2018), and distributed temperature measurement based on Raman scattering (Gorshkov and Taranov, 2018) and Mandelstam–Brillouin scattering (Sheng et al., 2021).

It took a little more than a decade for DAS technology to be commercialized in such areas as monitoring

**Table 1.** List of abbreviations most frequently used in distributed measurement literature

Notation:	Breakout
BFS	Brillouin Frequency Shift
BGS**	Brillouin Gain Spectrum
BOCDA**	Brillouin Optic Correlation Domain Analysis
BOCDR**	Brillouin Optic Correlation Domain Reflectometry
BOFDA**	Brillouin Optic frequency-Domain Analysis
BOFDR**	Brillouin Optic Frequency-Domain Reflectometry
BOTDA**	Brillouin Optic Time-Domain Analysis
BOTDR** (B-OTDR)	Brillouin Optic Time Domain Reflectometry
BP	Brillouin Pumping
CD	Chromatic dispersion
C-OFDR**	Coherent Optic Frequency-Domain Reflectometry
COR-OTDR (correlation OTDR)	Correlation Time-Domain Reflectometry
C-OTDR (CO-OTDR)	Coherent Optic Time-Domain Reflectometry
DAS**	Distributed Acoustic Sensing
DFOGS	Distributed Fiber Optics Geophysical Sensors
DFOS (DOFS)	Distributed Fiber Optic Sensing
DSS**	Distributed Strain Sensing
DSTS (DTSS**)	Distributed Temperature/ Strain Sensing
DTS	Distributed Temperature Sensing
DVS**	Distributed Vibration Sensors
EDFA	Erbium Doped Fiber Amplifier
FBA**	Fiber Brillouin Amplification
FBG	Fiber Bragg Grating
FMF	Few-Mode Fiber
FOSS	Fiber Optic Sensing System
FRA**	Raman Amplification in Fiber Optic Communication Systems
GL** (LG)	Gauge Length
MMF	Multimode Optic fiber
OCDR	Optic Coherence Domain Reflectometry
OFDR**	Optic Frequency Domain Reflectometry
OTDR** (TDR)	Optic Time Domain Reflectometry
POF	Plastic/Polymer Optic fibers
POFDR	Polarization Optic Frequency-Domain Reflectometry
POTDR (P-OTDR)	Polarization Optic Time Domain Reflectometry
PRF	Pulse Repetition Frequency
Raman OTDR	Raman optic time domain reflectometry
RBS	Rayleigh Backscattering Coefficient
RS	Rayleigh Scattering
SBS**	Stimulated Brillouin Scattering
SMF	Single Mode Optic fiber
SpBS**	Spontaneous Brillouin Scattering
SRS	Stimulated Raman Scattering
ULEB	Ultra-Low Loss-Enhanced Backscattering Fibers
$\Phi$ -OTDR** (phase OTDR)	Phase-Sensitive Optic Time Domain Reflectometry

\* Abbreviations are given that the authors encountered in publications without breakout.

\*\* Notation used in text of article.

of building structures (Aung et al., 2021; Bado and Casas, 2021), soil dams and embankments, slopes and landslides (Ivanov et al., 2021), ground subsidence and fracturing, as well as in security systems. DAS is increasingly used in vertical seismic profiling (Hull et al., 2019) and well monitoring (Keul et al., 2005; Daley et al., 2016; Shuvalov et al., 2018a; Yu et al.,

2019), in the exploration and production of oil and gas (for monitoring of multistage hydraulic fracturing) (Ning and Sava, 2018b; Borodin and Segal, 2020; Ichikawa et al., 2020; Wu Y. et al., 2020; Zhang Z. et al., 2020; Liu Y. et al., 2021a, 2021b). This technology is also used for seismic tomography of subsurface layers (Fernandez-Ruiz et al., 2020) and other appli-

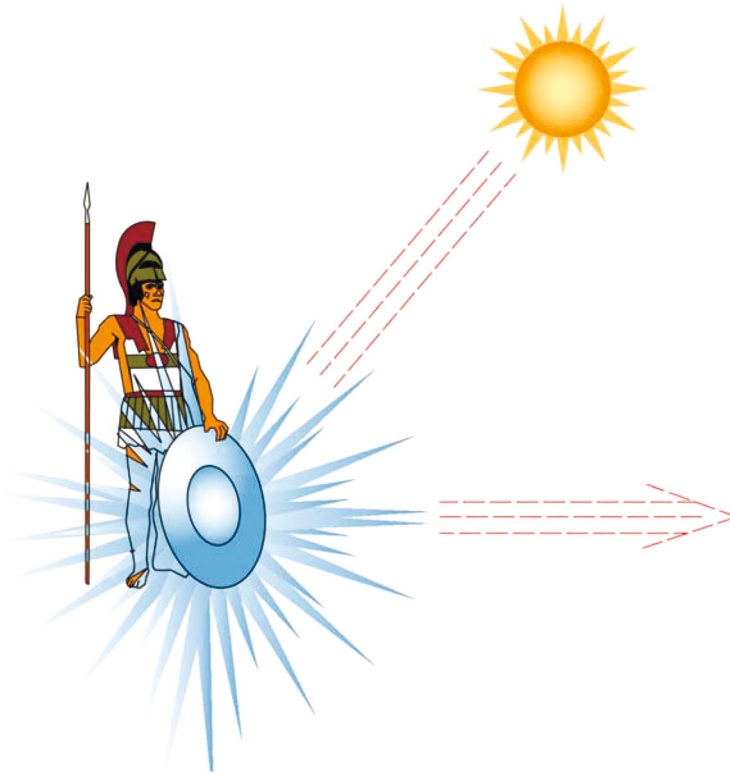


**Fig. 1.** Heliograph (signal with polished shield). The first mention is 490 BE.



**Fig. 2.** N.K. Roerich, “Flowers of Timur” (“Lights of Victory”). The picture shows the transmission of signals by bonfires.

cations. Why has this technology developed so rapidly, and what can be expected from it in the future? To answer this, let us examine what DAS is.

### *Fiber Optics*

To understand the operational principles of fibers, let us consider its two main elements: the core and

optic cladding (Fig. 5). The easiest way to describe passage of light through an optic fiber is in terms of geometric optics. Rays of light entering the core within a certain angle experience total internal reflection in the fiber and, as a first approximation, pass it to the end unchanged. The shortest path is the beam going through the center of the fiber, the lowest mode. The path of higher modes is longer, and this is the main

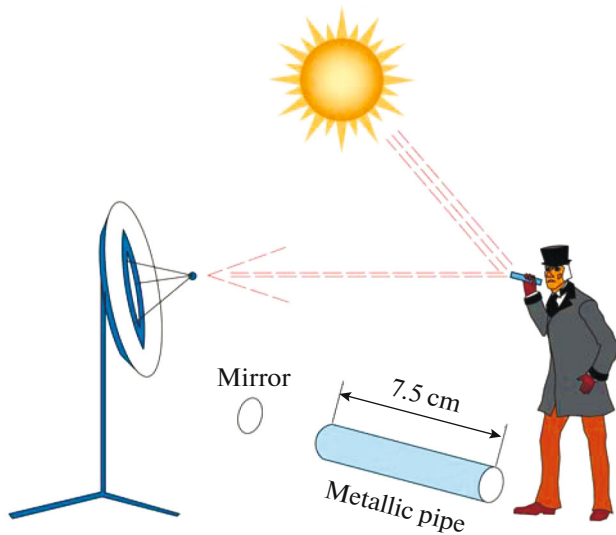


Fig. 3. Photophone by Alexander Graham Bell, 1878.

reason for the appearance of the pulse dispersion effect. Dispersion leads to distortion of the pulse shape, its broadening, and superposition of neighboring pulses, which limits the pulse transmission frequency. To avoid superposition of signals from adjacent pulses, their repetition rate  $f_i$  for distributed measurements should be limited by the time of flight of pulses in the fiber to the end of the operational length and return time of the scattered light to the starting point. It can be determined approximately as follows:

$$f_i = \frac{c}{n(2L + 2P + 3D)},$$

where  $c$  is the speed of light in vacuum,  $n$  is the refractive index of the fiber, which is assumed to be constant along its length,  $L$  is the operational length of the fiber,  $P$  is the length of fiber exposure to an undistorted light pulse,  $D$  is the pulse dispersion. The maximum readable frequency, according to the Nyquist theorem, is  $f_i/2$ .

The technology making it possible to gradually decrease the refractive index from the center of the fiber along the radius (multimode fiber with a gradient refractive index (Fig. 5b)) has made it possible to

Table 2. Stages leading to creation of DAS technology

Year	Event
1860s	Engineer V.N. Chikolev used light guides to illuminate powder magazines of Okhta gunpowder factory in St. Petersburg
1960	An article about the first laser has been published in the journal <i>Nature</i>
1965	First working fiber optic telecommunications
1976	Development of optic reflectometry
2010	Distributed acoustic sensing (DAS)



Fig. 4. Newton's rings (first description 1675).

reduce the dispersion. Since the speed of light in a medium increases with decreasing refractive index, rays traveling longer paths have greater speeds. A thin-core fiber allows single-mode operation (Fig. 5c). In such a fiber, the pulse undergoes the least distortion.

There are also more complex types of fibers: with shifted (zero) dispersion, flat dispersion, and dispersion compensation. They have a more complex refractive index profile, which is achieved by using multi-layer shells or special compensators.

Since already laid communication lines are often used for DAS, it is necessary to take into account the possibility of working with fibers of all types.

### LIGHT ATTENUATION IN A FIBER

Let us consider the reasons for the decrease in power of an optic signal as it passes through an optic fiber. This is primarily the radiation of leaky modes that do not fit into the angle of total reflection, and radiation at bends and microbends. Large losses may also be associated with splicing points of the optic fiber, where Fresnel reflection occurs when the refractive index changes and radiation by defects occurs. In no small way the light attenuation is related to light absorption by inclusions and the fiber material itself ( $\text{SiO}_2$  or a polymer). Some losses can be attributed to the fluorescence effect.

Conversely, DAS technology is based on light scattering, which assimilates a certain fraction of the energy of an electromagnetic wave and further emits this energy. Distributed measurements use light scattered back to its source. The scattering sources are optic inhomogeneities in the medium. When the sizes

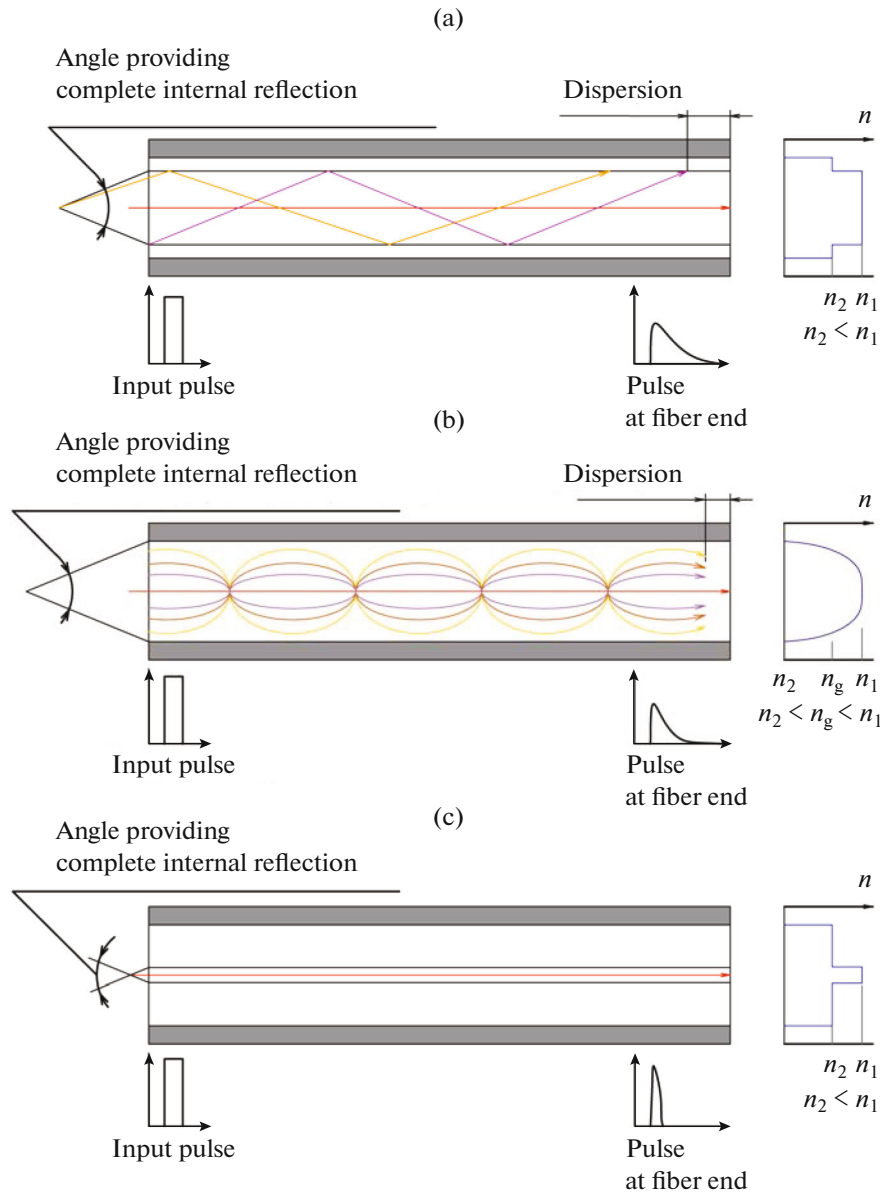


**Fig. 5.** Types of optic fibers: (a) multimode fiber with stepped refractive index; (b) multimode fiber with gradient refractive index; (c) single-mode fiber. Right: changes in refractive index along fiber diameter ( $n_g$  is group refractive index,  $n_1$  and  $n_2$  are refractive indices of fiber core and cladding, respectively); bottom: distortion of light pulse.

of inhomogeneities are comparable to the wavelength of the incident light or exceed it, we are usually dealing with Mie scattering. Such a relation of sizes implies account for the effects of wave interference, refraction, and diffraction; the scattering indicatrix assumes a complex shape, and sharp maxima and minima appear in it; moreover, such large defects and inclusions cannot be considered uniformly distributed over the volume of the fiber. This limits the possibility of using Mie scattering in DAS systems.

For distributed measurements, it is important that stray sources are approximately evenly spaced along the length of the fiber. This is how the inhomogene-

ities are distributed, from which Rayleigh scattering, Raman scattering, and Mandelstam–Brillouin scattering occur (Fig. 6). The effects on the fiber change the scattering characteristics, so, by analyzing the backscattered part of the light, it is possible to estimate these effects. By directly or indirectly influencing the propagation of light in a fiber, it is possible to detect fiber strain, determine temperature, measure the magnetic field (Faraday effect), electric field (Kerr effect), acoustic fields, rotation, humidity, and many other effects.

Note that the above definition of the Mie scattering, which is often found in the literature, is not

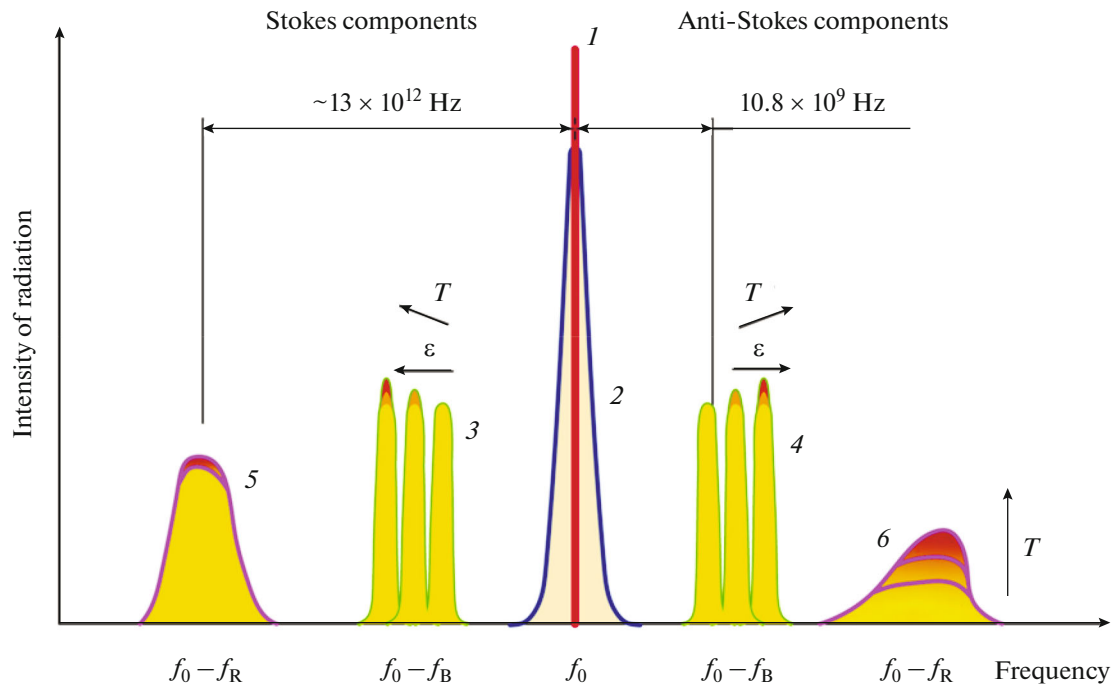


**Fig. 6.** Illustrative spectra of light scattering in optic fibers, taking into account influence of temperature ( $T$ ) and strain ( $\epsilon$ ). 1, Laser radiation at input; 2, Rayleigh scattering; 3, 4, Stokes and anti-Stokes Mandelstam–Brillouin scattering lines; 5, 6, Stokes and anti-Stokes lines of Raman scattering of light.

entirely correct. The Mie theory was developed for spherical particles with any ratio of sizes of inhomogeneities and wavelengths of light; therefore, Rayleigh scattering—the scattering of light by objects with dimensions much smaller than the wavelength—is a special case thereof. Like any Mie scattering, this is an elastic effect: the scattered light has the same wavelength as the transmitted light.

Raman scattering is inelastic scattering by the molecules of the medium, and the new frequencies in the scattering spectrum are combinations of the frequency of the incident light and frequencies of the vibrational and rotational transitions of the scattering molecules. Raman frequency shift  $f_R \sim 13$  THz. In scattered light, components appear with a lower frequency (Stokes) and higher frequency (anti-Stokes). The intensity of anti-Stokes components with frequency  $f_0 - f_R$  is significantly less than Stokes components  $f_0 f_R$ . The total intensity of the Raman scattered light is three to six orders of magnitude lower than the Rayleigh intensity. As the temperature increases, the intensity of the anti-Stokes lines increases significantly (in contrast to Stokes lines), which makes it possible to use this effect for distributed temperature sensing (Distributed fiber-optic..., 2022).

Mandelstam–Brillouin scattering is inelastic scattering of light during its interaction with thermal vibrations of the medium, which can be represented as quasiparticles (phonons) or refractive index waves. Stokes and anti-Stokes lines also appear in this scattering.

The intensity of Brillouin scattering for each of these lines is  $\sim 18$  dB lower than that of Rayleigh scattering, but an order of magnitude stronger than Raman scattering signals. The Brillouin frequency shift  $f_B$  is less than the Raman shift ( $\sim 11$  GHz); the generated bandwidths are very narrow ( $\sim 30$  MHz). Absolute temperature (and strain) sensing is possible due to the linear relationship between acoustic phonon energy and temperature (and strain) of fiber. The sensitivity to temperature of the anti-Stokes Mandelstam–Brillouin scattering lines is much lower than the same lines of Raman scattering.

Scattering of light in an optic fiber gives rise to the interference of waves scattered by individual particles between themselves and with the incident wave, and with increasing pulse power, the re-emission (multiple scattering) effect increases, when the light scattered by one particle is again scattered by others. With a high optic power density, the effects of stimulated scattering can occur: Raman and Mandelstam–Brillouin. The resulting nonlinear effects prevent a significant increase in the input radiation to increase the signal-to-noise ratio and increase the measurement range of the DAS.

#### *Monitoring of the Fiber Optic and Reflectometry*

Optic reflectometry is the measurement of reflection and backscattering in an optic fiber (Liokumovich et al., 2015; Iida et al., 2020); it was created to monitor

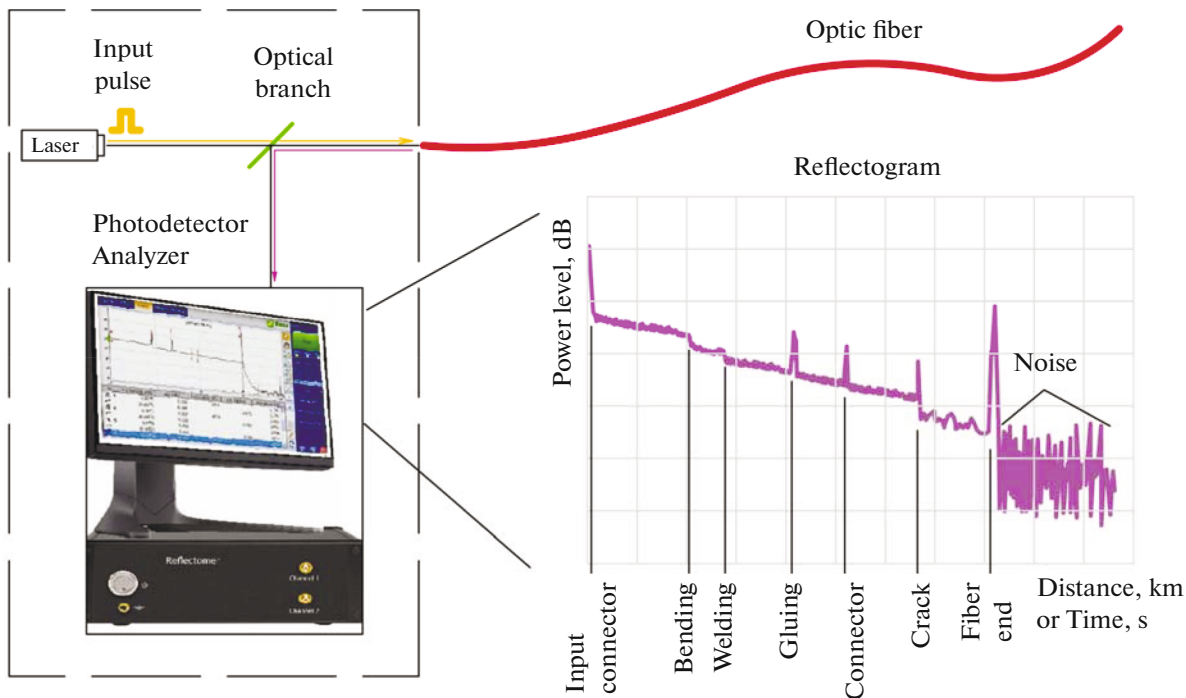


Fig. 7. Optical fiber inspection using reflectometer.

optic cables. A reflectometer makes it possible to reliably examine the parameters of the fiber, its defects, joints, breaks, damage, and inhomogeneities, as well as determine their location.

The principle of reflectometry resembles localization (Fig. 7). An optic pulse from a radiation source propagates in the studied fiber experiencing attenuation. Reflected backscattered and scattered radiation arrives at the photodetector, and a reflectogram is constructed. The slope of the curve is determined by the parameters of the fiber and wavelength of the radiation. The attenuation coefficient is measured in dB/km. Peaks in the reflectogram are caused by reflections within the fiber; dips are associated with losses.

If the location of a cable that gives a strong return signal is stretched or compressed, this will be noticeable on the reflectogram. However, this is not yet a distributed, but only a point measurement.

## DISTRIBUTED SEISMIC SENSING METHODS

For each specific seismometric task, several distributed sensing variants can be selected. The key parameters for choosing a variant are as follows: the operating length of the fiber on which measurements can be taken; discreteness of output seismic data (sampling rate); spatial resolution; frequency and dynamic ranges; single- or multimode fiber; whether there is access to only one end of the fiber or additional

access points are possible, etc. (Zhang J. et al., 2018; Wang Z. et al., 2020).

For measurements, light attenuation effects are used, which occur uniformly throughout the entire volume of the fiber and are sensitive to its axial strain (see Fig. 6). These are Rayleigh scattering (DAS systems) and Mandelstam–Brillouin scattering (DSS systems). Raman scattering is used only for distributed temperature sensing; nevertheless, Gorshkov et al. (2017) demonstrated the possibility of using it to measure the strain of an optic fiber.

With the aim of improving measurements, experiments and developments are constantly underway, and new commercial products are emerging (Buimistruk, 2005), so we do not present a numerical comparison of them.

DAS is usually implemented in one of the following schemes: OTDR (optic time domain reflectometry), which provides a higher sampling rate, or OFDR (optic frequency domain reflectometry). Sometimes the polarization and correlation properties of backscattering are also analyzed (Dashkov and Smirnov, 2018; Xiong et al., 2020).

OTDR, in turn, can be implemented in different ways (Fig. 8). The simplest configuration is to apply optic pulses to an optic fiber and measure the dependence of the scattered light intensity on the time delay between the introduction of the signal and fixation of its reflected part at the photodetector. Such a scheme finds almost no application due to the nonlinear non-monotonic dependence of the intensity on fiber strain.

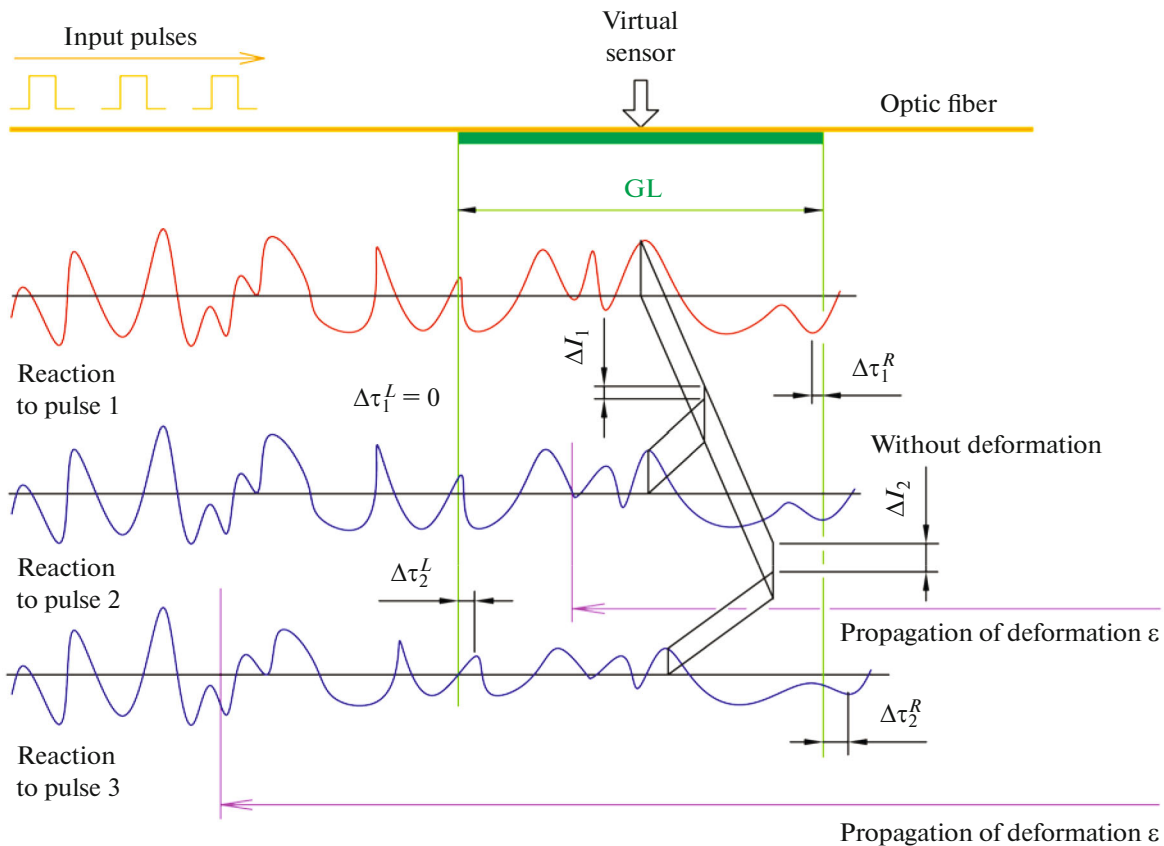


**Fig. 8.** Change in backscattering signal during fiber strain. Phase difference  $\Delta\tau_L - \Delta\tau_R$ , attributed to measuring length of GL, is proportional to tension/compression of fiber.  $\Delta I$ , Change in backscattered optic power.

The most commonly used is phase-sensitive optic time domain reflectometry ( $\Phi$ -OTDR) (Rao et al., 2021). It is assumed that the phase change is proportional to the axial strain of the fiber  $\epsilon$ , which can therefore be measured by phase demodulation methods or schemes that use information about the frequency shift in the probing pulses (Rohwetter et al., 2016; Muanenda, 2018; Alekseev et al., 2020; Soriano-Amat et al., 2021).  $\Phi$ -OTDR is optimal for solving problems requiring a combination of high sampling rates, resolution, and sensitivity when analyzing short and intermediate operating lengths in the frequency range from units of hertz to units of kilohertz.

Like any method, OTDR has its drawbacks, which include low measurement sensitivity; Rayleigh scattering phase fading (Gabai and Eysel, 2016); noise components of the system in the frequency domain, distorting the results; etc. For each problem, solutions have been developed (Alekseev et al., 2015; He et al., 2020a, 2020b; Liu Y. et al., 2021c; Zhang Y. et al., 2021). An indicator of the accuracy of  $\Phi$ -OTDR is the uncertainty of the measured phase shift (Alekseev et al., 2019). The inability to measure static or slowly changing effects somewhat narrows the scope of  $\Phi$ -OTDR.

If OTDR is supported by distributed Raman amplification (FRA) or Mandelstam–Brillouin scattering (FBA), an operating length of 150 km or more can be achieved (Chen et al., 2019; Distributed fiber sensors..., 2021).

As for OFDR, it is based on analysis of the interference signal between the initial signal and scattered signal in the fiber line during frequency scanning of the probing radiation. Implementation requires the a highly coherent tunable laser source. The signal obtained by scanning the frequency contains information about the exact position and magnitude of reflective events along the length of the fiber line and can be obtained, for example, using Fourier transform (Tkachenko et al., 2019). Some modifications of the method make it possible to obtain an operating length of up to 80 km with a data frequency of up to 5 kHz and a spatial resolution of 2.8 m or less (Gabai et al., 2015; Zhou et al., 2016; Kishida et al., 2021).

A promising scheme is coherent optic frequency domain reflectometry (C-OFDR) (Galkovski et al., 2021). In the simplest case, the source emits low-power light with an optic frequency that varies linearly with time. The light is divided into reference and test signals. The attenuation in the optic fiber creates a



characteristic backscattering profile, and the backscattering signal interferes with the coherent reference signal. Fast Fourier transform provides information about the frequency and specific amplitude of each virtual sensor on the fiber. Fiber deformation leads to a redistribution of scattering inhomogeneities, which changes the structure of OFDR traces and increases noise. Thus, the performance of this measurement method is limited by the low level of the soft clip.

DSS fiber sensors based on Mandelstam–Brillouin scattering can be constructed using both stimulated (SBS) (Coscetta et al., 2020) and spontaneous (SpBS) scattering. In both modes, the frequency shifts and powers of the Stokes and anti-Stokes components depend linearly on strain and/or temperature.

Mandelstam–Brillouin scattering is much weaker than Rayleigh scattering; to obtain the required measurement accuracy, it is necessary to process several pulses together. Thus, the maximum output data frequency is typically a few tens of hertz. Conversely, in contrast to SBS, reflectometry based on spontaneous Mandelstam–Brillouin scattering makes it possible to query the measuring system using only one end of the fiber optic line.

SPS is caused by a change in particle motion under the influence of the incident light wave (Minardo et al., 2021). In this case, oppositely directed light pulses are used. This approach requires laying a double fiber with a loop or at least mirror reflection at the end point. Stimulated scattering occurs when the frequency difference of the counterpropagating waves is close to the phonon frequency. Due to electrostriction, these waves cause a traveling acoustic wave, which increases the phonon population. From the intensity of the reflected optic pulse and the time of its passage, one can determine the profile of the Brillouin frequency shift along the fiber. When measuring temperature, such circuits have an advantage over Raman sensors, since they use a stronger signal. To obtain the Brillouin gain spectrum (BGS), the frequency shift between the pump and test beams must be scanned; data averaging is also required here. It is usually necessary to use several dozen gain profiles in order to reconstruct the temperature or strain distribution along the fiber with proper accuracy.

Unlike DAS, DSS directly responds to deformation, so it is used for quasi-static measurements in the monitoring of bridges, tunnels, pipelines and building structures (Barrias et al., 2016). Like Rayleigh scattering methods, DSS can be implemented in a variety of ways.

BOTDR (Brillouin optic time domain reflectometry) determines the distribution of mechanical loads on the fiber by the delay between the Brillouin shift and the modulated pump pulse (Fiber-optic..., 2022). Spontaneous Brillouin scattering (SpBS) is most commonly used. In some types of BOTDR, short pump pulses of monochromatic radiation are autohet-

erodyned with backscattered light, causing the SBS effect.

BOFDR (Brillouin optic frequency domain reflectometry) measures strain and/or temperature along a single access optic fiber, detecting spontaneous Brillouin scattering. The operating principle of BOFDR is very similar to BOTDR, except for the use of sinusoidally modulated, rather than pulsed pump light (Minardo et al., 2016).

In BOCDR (Brillouin optic correlation domain reflectometry) technology, continuous laser radiation is modulated with a sinusoidal signal. Part of the light directed into the fiber under study undergoes scattering and returns to the beginning of the fiber with a shifted frequency. The autoheterodyne method of mixing with the reference part of the laser radiation creates a beat signal. A modulating sinusoidal signal is chosen at such a frequency that the coherence function reaches its maximum only once for a given operating length of the fiber (one beat). Using a spectrum analyzer, the Brillouin frequency shift corresponding to this segment of the fiber is obtained. By changing the parameters of the laser radiation modulation, it is possible to scan the entire operating length of the fiber (Mizuno et al., 2018; Tangudu and Sahu, 2020).

Methods using SBS are called Brillouin scattering analysis systems. Because SBS is much stronger than SpBS, the signal-to-noise ratio for these methods is much higher, resulting in short measurement times due to fewer averages. However, SBS requires two-way fiber access, which is not always possible.

BOTDA (Brillouin optic time domain analysis) requires two lasers, the radiation of which—probing and pump—are directed oppositely along the fiber. One laser (in principle, it does not matter which) is continuous, while the other is pulsed. SBS occurs in fiber sections that are simultaneously illuminated by the pump and probing light. This causes signal amplification that can be detected and located. In order to determine the profile of local shifts of the Brillouin frequency and hence the deformation (or temperature) along the fiber, it is necessary to change (swing) the optic frequency of one of the lasers (Motil et al., 2016).

BOFDA (Brillouin optic frequency domain analysis) uses a sinusoidally modulated pump beam. BOFDA transducers have good spatial resolution (centimeters or even millimeters for short operating lengths). At a lower resolution, the operating length can be more than 100 km or more (Kapa et al., 2019). The output sampling rate of this method is better than that of BOTDA.

BOCDA (Brillouin optic correlation domain analysis) is based on frequency modulation of opposing light sources in order to activate SBS in a fiber segment; i.e., random access can be implemented to several points that are selected along the fiber (Denisov et al., 2016).

In parallel distributed temperature and strain sensing (DTSS), the frequency shift and powers of the Stokes and anti-Stokes components of scattered radiation are determined simultaneously. However, the sensitivity characteristics of such systems are insufficient in most cases; therefore, more complex measurement schemes are used. Temperature and strain can also be separated by laying two fibers, one of which is laid loose (not subject to tension/compression effects) and only measures temperature.

Separation of strain and temperature is convenient for parallel or mixed application of methods based on scatterings of different nature. In this case, one or more fibers can be used (Zhou et al., 2013; Peng and Cao, 2016).

### *What Are We Measuring?*

The main advantage of distributed sensing is the high density of virtual sensors conventionally placed along the fiber. Each sensor corresponds to a certain segment, called the gauge length (GL); the middle of the GL is considered its location. The GLs of adjacent sensors may overlap. In most DAS schemes, the signal is formed based on the phase difference between two points on the reflectogram corresponding to the edges of the GL. It is what happens at the ends of the GL that actually determines the output. A small GL degrades the signal-to-noise ratio, while a large one can cause signal distortion. The appropriate GL is selected based on the signal-to-noise ratio and signal wavelength (Dean et al., 2017; Alfataierge et al., 2020). DAS data are quite different from those obtained from traditional seismometers.

First, most of the methods traditionally used to analyze seismic data are based on in point measurements. Secondly, DAS produces records of strain or strain rate, while it is customary to rely on the kinematic components of the Earth's motion for solving many problems, i.e., displacements, velocities, or accelerations. Many have attempted to reduce DAS measurements to these (Wang H.F. et al., 2018; Lindsey et al., 2020; Lior et al., 2020, 2021a, 2021b; van den Ende and Ampuero, 2021).

To some extent, the DAS measurement can be represented as the difference between the readings of two traditional seismometers (for example, velocimeters) located at the extreme points divided by GL. The DAS record should approximate the strain gage transducer (with a length GL) that measures fiber strain starting at quasi-static frequencies. Reconstruction of traditional sensor readings from DAS records is feasible, but it should be borne in mind that this approach is mathematically incomplete. Based on the calculations given in (Chambers, 2022), it is possible to construct theoretical dependences of the DAS amplitude response on frequency and angle of incidence  $\alpha$  (Figs. 9, 10).

Thus, in addition to the usual attenuation of a seismic signal with distance, it is necessary to take into account the angle of incidence on the fiber, GL, and change in the frequency content. Lower frequencies attenuate due to the smaller difference in signals at the extreme points of the GL. For perpendicular wave incidence (angle of incidence  $90^\circ$ ), the absence of a DAS response to the *S*-wave is because in this case, there is no relative movement between the ends of the GL. Thus, the sensitivity of a horizontally placed fiber of the DAS to vertical perturbations is zero. This is particularly important for teleseismic *P*-waves, since they propagate almost vertically near the surface.

Another important difference between distributed sensing is that in many schemes, in order to achieve the required accuracy, it is necessary to average the readings over several pulses. Traditional seismometers, being analog in nature, produce instantaneous measurements, while DAS measurements can no longer be considered instantaneous. A new metrological characteristic is introduced: time of measurement.

An individual direction in developing DAS is the organization of its own seismic lines, in which the fibers have an exact orientation, location, and calculated connection with the ground. For them, special cables are being developed that have a better signal-to-noise ratio and good transmission of the impact on the fiber while maintaining mechanical protection (Han et al., 2021; Van Putten et al., 2021). Since BFS sensors are sensitive to both temperature and strain, fibers are being developed that have widely differing frequency response factors, which allows the cause of frequency variations to be disambiguated. Of course, special fibers have a significantly higher cost.

DAS is a one-component system, so there is a circumferential uncertainty in determining the direction of signal arrival. It should also be taken into account that the location of each segment of the fiber and its direction are not always known with sufficient accuracy. This is particularly true for DAS systems that use existing telecommunication lines (Huot and Biondi, 2018). DAS virtual seismic instruments are calibrated using test signals (e.g., sledgehammer strikes (Klaasen et al., 2022)), and if this is inefficient or impossible, procedures using data from closely spaced traditional seismometers (Paitz et al., 2020).

Determination of orientation and calibration are fairly common tasks in seismometry: the response of a traditional single-component seismometer to movements also depends on the angle of incidence of the wave on the sensitivity axis, and its response is frequency-dependent. Downhole seismometers also require positioning and orientation.

The farther from the starting point, each next virtual sensor has a lower signal-to-noise ratio. In addition to this general trend, the instrument response depends on many factors, including local environ-

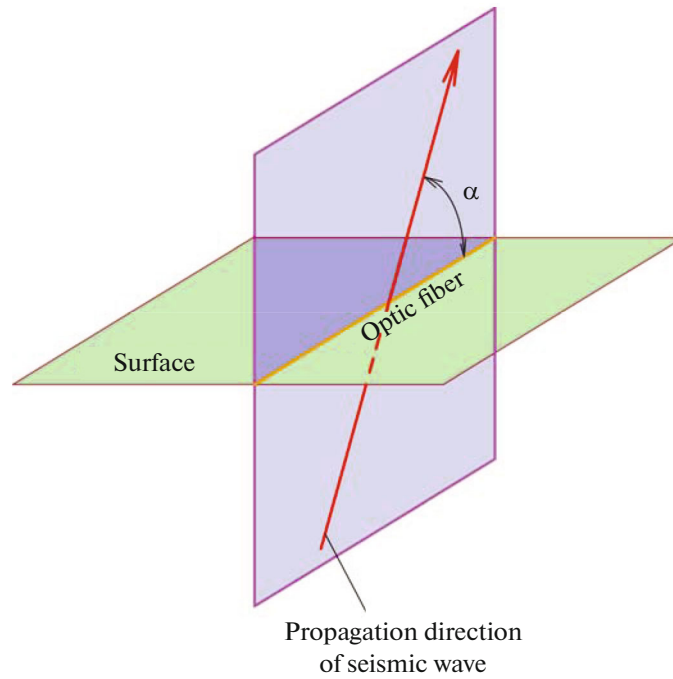


Fig. 9. Diagram of seismic wave propagation during DAS observations.  $\alpha$ , angle of incidence of wave on fiber.

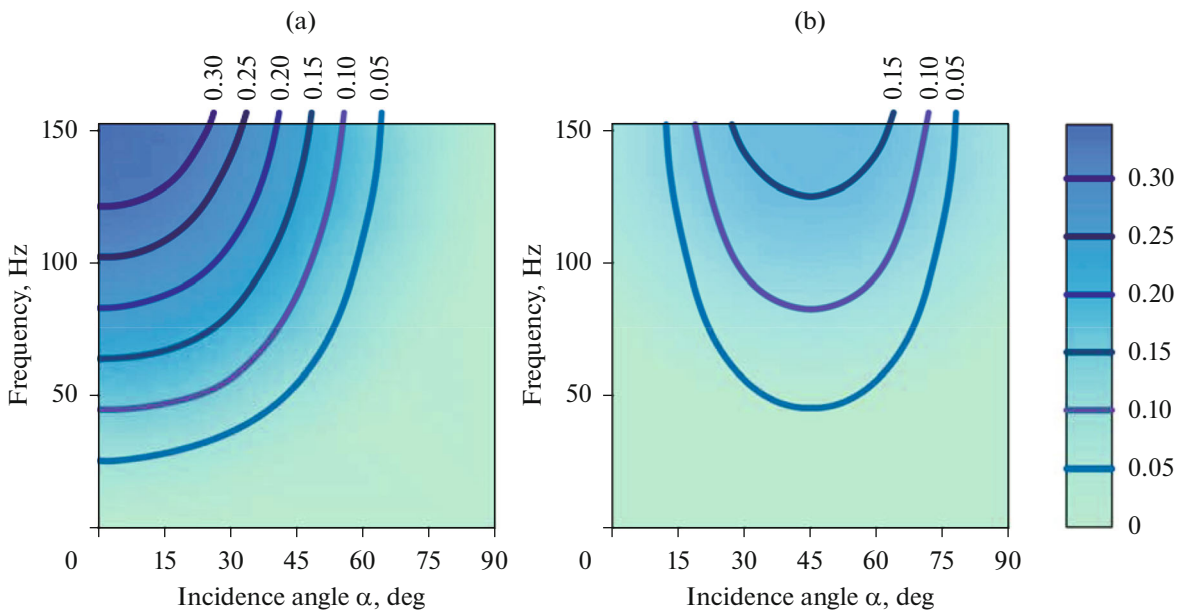


Fig. 10. Amplitude response (scale on right) of virtual sensor, characterizing deformation, depending on angle of incidence and frequency of seismic signal: (a) for  $P$ -wave; (b) for  $S$ -wave. In calculations, seismic waves were considered planar.  $GL=10$  m, velocity of  $P$ -wave  $V_P=2500$  m/s, velocity of  $S$ -wave  $V_S=1560$  m/s.

mental properties, cable design (Chapeleau and Basil, 2021), and its installation method.

Distance along the fiber  $z$  from the polling unit to the virtual sensor is determined by time  $t$  of the signal return:  $z(t) = ct/2n$ , where  $c$  is the speed of light in vacuum;  $n$  is the refractive index of the fiber.

### Cable Laying

The key parameters that affect the metrological performance of DAS are the cable design and installation method. The stiffer the cable, the lower its sensitivity. Poor communication with the ground greatly changes the transient function: it reduces the signal-

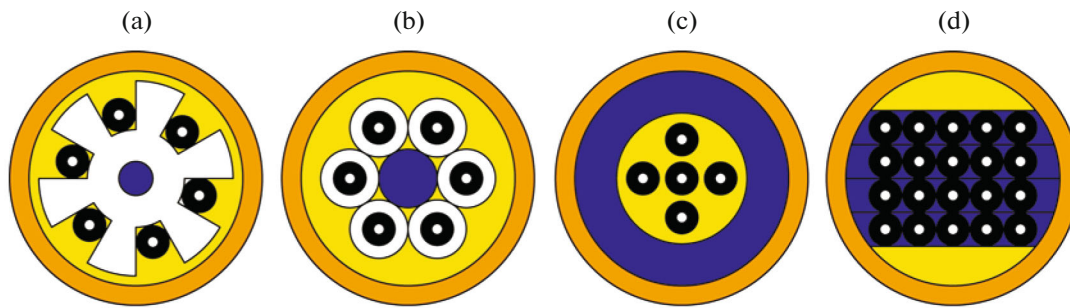


**Fig. 11.** Designs of optic cables for communication systems. (a) Cable with profiled core; (b) modular cable; (c) cable with central module; (d) ribbon cable. Optic fibers and reinforcing and protective elements are often twisted (like electrical cables) with different pitches and lay directions within single cable; ribbon package is twisted in spiral.

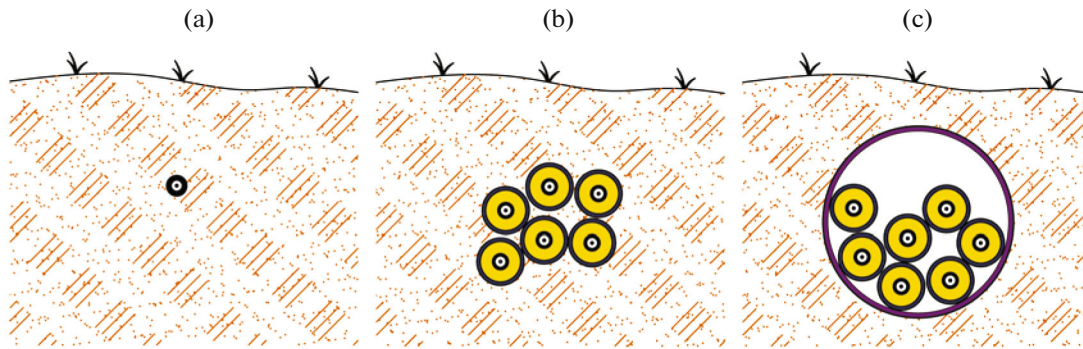


**Fig. 12.** Some underground laying methods for optic cables. (a) Laying cable into ground; (b) instillation in PVC pipe with diameter of about 6 cm, filled with hydrophobic gel; (c) combination of several pipes in common casing.

to-noise ratio and affects the frequency content of the recorded signal (Papp et al., 2017).

Fiber optic lines can be underground, underwater, overhead, or combined cables. They have various design, and a different connection with the ground is possible (Reinsch et al., 2017; Becker et al., 2018) (Figs. 11, 12). The best performance is yielded by a single single-mode fiber with minimal protection, buried in the ground even to a shallow depth. Clearly, however, this variant is not very good for long-term experiments.

For vertical DAS systems, various methods are used to connect the DAS cable to the ground (Correa et al., 2019; Lellouch and Biondi, 2021; Zhang C. et al., 2021). The cable can simply be lowered into a borehole for the duration of the experiment. This is the worst option in terms of its contact with the ground, but it allows the use of existing boreholes. Other options involve rigidly attaching the cable permanently to the outside of the pipe, which makes it possible to use DAS without shutting down the borehole and, given the durability of the cable and its low cost, is the best option.

If the cable is laid underwater, then its fixation to the ground depends on the bottom sediments, the bot-

tom relief and the laying method. There are cases when the cable simply sags over a trough bottom; however, such sections are quite easily determined from the signal record (Sladen et al., 2019).

#### ADVANTAGES OF DAS

The main advantage of DAS is its unprecedented high spatial resolution. In seismological applications, virtual sensors are usually calculated with a resolution on the order of several meters, but it can also be centimeters. At the same time, depending on the problem, the GL and discreteness of the sensors can be changed using the same primary data. One fiber optic cable can simultaneously act as several seismic arrays operating in different frequency ranges, from kilo- to millihertz (Ide et al., 2021; Shragge et al., 2021). The dynamic range exceeds 120 dB.

The operating length of the fiber can be tens of kilometers (Awwad et al., 2020) (Table 3). The main limitation is that, as the distance from the beginning of the cable increases, the noise increases.

An important advantage of DAS is that existing telecommunications cables can be used for seismological applications. So-called “dark fibers” are always

**Table 3.** Typical parameters of the most commonly used distributed sensors

Parameter	Meaning
Physical principle	Rayleigh scattering
Signal reception method	Optic time domain reflectometry – OTDR
Measurements	Phase (axial fiber strain) or phase change (strain rate)
Laser wavelength	1550 nm/s
Pulse duration	10–40 ns
Fiber exposure length	1–4 m
Pulse frequency	2–100 kHz
GL	10 m
Operating length of fiber	~50 km
Positioning accuracy of virtual sensor	1 m
Refractive index of fiber core	1.468
Single-mode fiber attenuation	0.2 dB/km (min 0.154 dB/km)
Fiber diameter	125 $\mu$ m
Fiber weight	~30 g/km
Minimum allowable fiber bend radius	2 mm
Fiber tensile strength	~7 kg
Frequency of digitized seismic signal	100–1000 Hz
Data volume	0.01–10 TB/day
Temperature range of fiber use (the temperature range of the cable is determined by its design)	–270 to +1000°C
Rated input power	80 W
Life time	>15 years

structurally laid in them, designed to expand the volume of communications and replace failed ones. Due to the low cost-intensity, the fibers are laid in excess. The use of these dark fibers in no way interferes with the function of the cable for its intended purpose. We add that old abandoned and even broken cables can be used for DAS; the main thing is that the segment of the required length from the beginning is intact. DAS technology enables rapid deployment and data collection with minimal new hardware. The DAS system can be operated continuously for many years with real-time data transmission or temporarily installed on a cable for surveying the area or any experiments.

Fiber optic cables are reliable and have a long service life. They are insensitive to electromagnetic fields and do not themselves generate external electromagnetic radiation. Cables can be operated at temperatures from –60 to +250°C and pressures up to 180 MPa, and specially designed cables, even under more severe conditions. Separate virtual sensors do not require power and maintenance; there is no synchronization problem between them; all that is required is an interrogator located at one end of the fiber in a convenient location. The high sampling rate of the signal eliminates aliasing. Cables used for seismological applications are much easier to install in inconvenient or hard-to-reach places than it is to orga-

nize a seismic network based on traditional instruments. Such places include the bottom of the sea, the slopes of volcanoes (Currenti et al., 2020), glaciers (Booth et al., 2020; Hudson et al., 2021), metropolitan areas (Fang et al., 2020; Spica et al., 2020b). DAS systems can easily be deployed in seismically inactive regions, usually with a very sparse seismic network. On the seafloor, distributed measurements can be used to indirectly study other processes such as volcanic activity, tsunamis, slope failure, sediment transport, etc. (Spica et al., 2020a; Taweessintananon et al., 2021).

For some applications, such as well monitoring, the possibility of parallel distributed temperature recording is also important.

The DAS data are suitable for many geophysical applications (Shuvalov et al., 2018b; Reinsch et al., 2020; *Distributed Acoustic Sensing...*, 2021), such as source localization, complete waveform inversion (Faucher et al., 2021), and tomography, as well as for studying the small-scale structure of the crust and upper mantle, analyzing surface waves, etc. (Nayak and Ajo-Franklin, 2021b). Given the prospects for development of this technology, it is difficult even theoretically to limit the possibilities of its application (Yu et al., 2019). At the same time, the data are easily visualized and interpreted.

We also mention the wide availability and prevalence of source materials, ease of deployment and low cost.

## PROBLEMS

Naturally, this new technology has unresolved problems. Currently, DAS can be implemented on a cable (cable segment) of only a limited length; thus, the media-circulated information that distributed sensing can be done over the entire length of transoceanic communication lines is a myth (Fu et al., 2018). So far, the operating length of distributed sensing achieved does not exceed 175 km (Wang Z.H. et al., 2014).

Longer distances can be achieved with dedicated optic repeaters and multistage distributed amplification along the fiber line. A similar principle is used in telecommunication lines. Every 50 km, there is an optic repeater, powered by an electrical cable laid along with the optic fiber. However, two-way transmission is technically difficult outside the optic amplifier and especially outside the repeater, where the signals are converted to electrical signals, processed, converted back to optic signals, and transmitted further.

As noted, DAS records only axial strain of the fiber; i.e., it is a uniaxial sensor. All-around uncertainty is combated by using cable bends as differently oriented sensors, by criss-crossing several fibers, or by using nearby conventional seismometers. Specially designed cables (Hornman, 2017) are used, as well as multicomponent sensing, i.e., several parallel fibers with different characteristics (Ning and Sava, 2018a), etc.

The dependence of the DAS response on the angle of incidence of a seismic wave can be overcome by jointly processing data from individual sensors (Bakulin et al., 2017; Liang et al., 2019). Spiral winding of the fiber is also a known method (Kuvshinov, 2016; Abbott et al., 2019).

The type of fiber optic cable (Zhang C. et al., 2020) and installation procedures (Becker et al., 2017) can also affect the DAS amplitude response. The transfer function can be calibrated using a broadband seismometer (Lindsey et al., 2020); however, this procedure is repeated for each application of distributed metering. There is no single standard for calibrating the DAS transfer function yet. The geographic coordinates of virtual sensors are difficult to determine, especially on previously laid cables.

An individual virtual sensor has a higher noise level than a conventional broadband seismometer. This limits the ability of DAS to detect weak signals (Foster, 2021). The signal-to-noise ratio can be improved by using special cables. The self-noise of DAS has not been rigorously evaluated at present; the signal-to-noise ratio of different segments of the cable is differ-

ent and decreases with distance from the polling unit. In addition, existing communication cables are usually laid in noisy places. The use of DAS as an array can partially mitigate this drawback, especially since cables usually do not run in a straight line; i.e., the direction of sensitivity from one virtual sensor to another varies.

As mentioned above, the connection between the fiber optic cable and ground varies along the length of the cable due to differences in soil type and installation method; thus, the transfer function of different cable segments is different. The complete transfer functions of fiber optic systems are not defined and also depend on the angle of incidence, the frequency content of the signal, and the thickness of the fiber.

DAS can only detect and localize a perturbation; however, using DAS to estimate the magnitude and focal mechanism remains an open question. The suitability of conventional seismological methods for processing seismic arrays requires careful assessment.

It should also be noted that the metrology of measurements, to put it mildly, is rather poor.

There are difficulties associated with the physics of the method and imperfection of the measurement algorithms. This can include dispersion, i.e., time dispersion of the spectral or mode components of the interrogation pulse. Another notable disadvantage is signal fading, which causes the signal from some segments of the cable (some virtual sensors) to drop below the noise level (He et al., 2020b). To counter this phenomenon, pulse chirping and a set of pulses of different frequencies are used (Masoudi and Newson, 2016; Pastor Graells et al., 2016; Yatsev et al., 2019). Pulses of different shapes are also used, including triangular, rectangular, Gaussian, and super-Gaussian, with the same total pulse energy (Fernandez-Ruiz et al., 2016).

## APPLICATIONS

Already, DAS has been successfully used in a variety of geophysical applications (Lellouch et al., 2021a). The use of DAS in exploration and production of minerals is widely known; it has been commercialized, reflected in a large number of publications (Binder et al., 2020; Hartog, 2020; Lellouch et al., 2020; Naldrett et al., 2020). We should also mention monitoring of building structures (Fernandez et al., 2021), used in engineering geophysics. Other DAS applications are also possible in this field, up to imaging of seismic noise and the wave fields of megacities (Matsumoto et al., 2021; Song et al., 2021b). Many aspects of seismic array technology, such as beamforming (Bakulin et al., 2018; Luo et al., 2020; Verdon et al., 2020; Yuan S. et al., 2020; Lellouch et al., 2021b; Nayak and Ajo-Franklin, 2021a) are also easily applicable to distributed sensing data.

So far, passive and active high-resolution seismic tomography and monitoring of microearthquakes are

being carried out in experiments (Baird et al., 2020; Huff et al., 2020), as well as study of the small-scale structure of the crust and upper mantle (Dou et al., 2017). Reliable source localization will undoubtedly be useful in studying aftershocks and earthquake swarms.

This technology is very promising for rapid seismic observations (e.g., for studying aftershocks) (Li et al., 2021). DAS is applicable for surveying areas of weak seismicity and places where organization of traditional observation points is difficult (Booth et al., 2020; Smolinski et al., 2020; Klaasen et al., 2021).

Detailed monitoring of the cryosphere, which earlier presented certain difficulties (Kislov and Gravirov, 2021) is now quite accessible (Wagner et al., 2018; Walter et al., 2020). In this case, distributed temperature monitoring is also possible.

A natural application of distributed sensing is marine geophysics (Min et al., 2021), including fault mapping, studying their movements (Shinohara et al., 2020; Cheng et al., 2021), determination of sedimentary rock distribution on the shelf, and analysis of oceanic microseisms and tides.

DAS is finding application in monitoring earthen dikes and embankments, slopes and landslides, ground subsidence, and fractures (Kreber, 2022). Works on monitoring CO<sub>2</sub> reservoirs and geothermal research are also known (Parker et al., 2018; Wuestefeld and Weinzierl, 2020; Popik et al., 2021; Tribaldos and Ajo-Franklin, 2021), as well as seismic assessment of construction sites, and early warning of tsunamis and earthquakes.

In addition to geophysics, DAS technology is applicable in perimeter protection, measurement and monitoring of ocean currents and infrasound, storm detection, acoustic wave propagation, mapping of underground structures, defect detection, monitoring of pipelines, railways, and power lines, traffic detection, and location of submarines and drones. In almost any industry that requires monitoring of an extended object, an optic cable can be used as a sensor.

The use of DAS during missions to other planets is very promising, since the system makes it easy to organize a dense array of broadband seismic stations; it also features low weight, volume, and power consumption (Martins et al., 2016).

Except the last one all other applications of this technology have already been implemented in practice, although in most cases only in pilot research experiments.

## DEVELOPMENT DIRECTIONS

The developers of equipment, measurement algorithms, and data processing programs still face many challenges. Now the capabilities of DAS are sufficient for modeling the velocities of a seismic wave field, for example, during vertical seismic profiling (Mateeva

et al., 2017; Bellefleur et al., 2020; Kobayashi et al., 2020; Lund et al., 2020; Pevzner et al., 2020; Titov et al., 2021), ambient noise velocity inversions (Ajo-franklin et al., 2019), determining the phase of an earthquake (Lindsey et al., 2017; Jousset et al., 2018), source localization, and other problems (Song et al., 2021a). However, measurements of ground motion amplitudes are necessary for solving many seismological problems, including total waveform inversion, moment tensor inversion, attenuation analysis, etc. Correct measurements of the true amplitudes of ground motion is a natural development goal for DAS.

The metrology should be developed, including intercalibration methods for DAS and conventional seismometers with the possibility of joint operation.

Hardware developments include low-noise optic fibers specialized for DAS, increasing the operating length (Xue et al., 2021), and cable laying methods. It is possible to develop dual-purpose communication cables that include DAS. The main thing here is the presence in the cable of local polling units, optic repeaters, and amplifiers that serve as DAS. Conversely, there should be interrogators that can be easily and quickly connected to communications with any type of fiber, and of course, DAS should be a simple tool to easily receive data without the need for one to become a specialist in fiber optics, laser technology, etc.

## DISCUSSION

In addition to individual DAS lines, seismic networks are convenient to use, combining several cables, including vertically placed (downhole) cables, which yield a full three-dimensional image. Multidimensional wavefield analysis provides information that cannot be extracted using traditional methods. This will serve to enrich catalogs, open up new possibilities for determining wave velocities, dispersion curves of seismic events, etc. Both horizontal fiber and downhole vertical DAS systems can complement existing LANs.

There is one more problem. If each DAS system of sufficient length will provide several terabytes of data per day, they will need to be somehow processed, archived, and stored with the possibility of future use (Dong et al., 2020). Already, an artificial intelligence apparatus is being used to process data from various DAS experiments (Fedorov et al., 2016; Li and Zhan, 2018; Binder and Chakraborty, 2019; Jia et al., 2019; Shi et al., 2019; Wang Z. et al., 2019; Jestin et al., 2020; Stork et al., 2020; Wu H. et al., 2020; Kye et al., 2021; Wamriev et al., 2021; Lv et al., 2022). This work should also be expanded.

## CONCLUSIONS

The development of DAS in the near future will make it possible to obtain high-quality data for almost

any seismological task. The large amount of data presumes the use of artificial intelligence. Only such a combination of technologies will make it possible, first, to simply use the data, and second, to extract the necessary knowledge from them.

With a high probability, it can be suggested that, in the next five years, there will be a paradigm shift in theoretical seismometry and even seismology in general.

In the future, the development of fiber optics will significantly complement the capabilities of fiber optic sensors, optic information processing methods will become available without optoelectronic conversion, and the use of optic information processing based on neural network decision-making.

#### FUNDING

The study was carried out within the state tasks of the Institute of Earthquake Prediction Theory and Mathematical Geophysics, Russian Academy of Sciences, and the Schmidt Institute of Physics of the Earth, Russian Academy of Sciences.

#### CONFLICT OF INTEREST

The authors declare that they have no conflicts of interest.

#### REFERENCES

- Abbott, R.E., Mellors, R., and Pitarka, A., Distributed acoustic sensing observations and modeling of the DAG series of chemical explosions, *CTBT: Science and Technology*, Vienna, Austria, 2019, T.23–P12.
- Ajo-Franklin, J.B., Dou, S., Lindsey, N.J., Monga, I., Tracy, C., Robertson, M., Tribaldos, V.R., Ulrich, C., Freifeld, B., Daley, T., and Li, X., Distributed acoustic sensing using dark fiber for near-surface characterization and broadband seismic event detection, *Sci. Rep.*, 2019, no. 9, p. 1328.  
<https://doi.org/10.1038/s41598-018-36675-8>
- Alekseev, A.E., Vdovenko, V.S., Gorshkov, B.G., Potapov, V.T., and Simikin, D.E., A phase-sensitive coherence reflectometer with amplitude-phase modulation of probing pulses, *Tech. Phys. Lett.*, 2015, vol. 41, pp. 72–75.  
<https://doi.org/10.1134/S1063785015010174>
- Alekseev, A., Gorshkov, B., and Potapov, V., Fidelity of the dual-pulse phase-OTDR response to spatially distributed external perturbation, *Laser Phys.*, 2019, vol. 29, no. 5, p. 055106.  
<https://doi.org/10.1088/1555-6611/ab0d15>
- Alekseev, A.E., Gorshkov, B.G., Potapov, V.T., Taranov, M.A., and Simikin, D.E., Dual-pulse phase-OTDR response to propagating longitudinal disturbance, *Laser Phys.*, 2020, vol. 30, no. 3, p. 035107.  
<https://doi.org/10.1088/1555-6611/ab70b0>
- Alfataierge, E., Aldawood, A., Bakulin, A., Stewart, R., and Merry, H., Influence of gauge length on DAS VSP data at the Houston Research Center test well, *90th Ann. Int. Meeting, SEG 2020: Expanded Abstracts*, 2020, pp. 505–509.  
<https://doi.org/10.1190/segam2020-3419066>
- Aung, T.L., Ma, N., Kishida, K., and Guzik, A., Advanced structural health monitoring method by integrated isogeometric analysis and distributed fiber optic sensing, *Sensors*, 2021, vol. 21, no. 17, p. 5794.  
<https://doi.org/10.3390/s21175794>
- Awwad, E., Dorize, C., Guerrier, S., and Renaudier, J., Detection-localization-identification of vibrations over long distance SSMF with coherent  $\Delta\phi$ -OTDR, *J. Light-wave Technol.*, 2020, vol. 38, no. 12, pp. 3089–3095.  
<https://doi.org/10.1109/JLT.2020.2993167>
- Bado, M.F. and Casas, J.R., A review of recent distributed optical fiber sensors applications for civil engineering structural health monitoring, *Sensors*, 2021, vol. 21, no. 5, p. 1818.  
<https://doi.org/10.3390/s21051818>
- Baird, A.F., Stork, A.L., Horne, S.A., Naldrett, G., Kendall, J.-M., Wookey, J., Verdon, J.P., and Clarke, A., Characteristics of microseismic data recorded by distributed acoustic sensing systems in anisotropic media, *Geophysics*, 2020, vol. 85, no. 4, pp. KS139–KS147.  
<https://doi.org/10.1190/geo2019-0776.1>
- Bakulin, A., Golikov, P., Smith, R., Erickson, K., Silvestrov, I., and Al-Ali, M., Smart DAS upholes for simultaneous land near-surface characterization and subsurface imaging, *Leading Edge*, 2017, vol. 36, no. 12, pp. 1001–1008.  
<https://doi.org/10.1190/tle36121001.1>
- Bakulin, A., Golikov, P., Erickson, K., Silvestrov, I., Kim, Y.S., Smith, R., and Al-Ali, M., Seismic imaging of vertical array data acquired using smart DAS uphole acquisition system, *SEG Technical Program Expanded Abstracts*, 2018, pp. 4050–4054.  
<https://doi.org/10.1190/segam2018-2995404.1>
- Bakulin, A., Silvestrov, I., and Pevzner, R., Surface seismics with DAS: An emerging alternative to modern point-sensor acquisition, *Leading Edge*, 2020, vol. 39, no. 11, pp. 808–818.  
<https://doi.org/10.1190/tle39110808.1>
- Barrias, A., Casas, J.R., and Villalba, S., A review of distributed optical fiber sensors for civil engineering applications, *Sensors*, 2016, vol. 16, no. 5, p. 748.  
<https://doi.org/10.3390/s16050748>
- Becker, M.W., Ciervo, C., Cole, M., Coleman, T., and Mondanos, M., Fracture hydromechanical response measured by fiber optic distributed acoustic sensing at millihertz frequencies, *Geophys. Res. Lett.*, 2017, vol. 44, no. 14, pp. 7295–7302.  
<https://doi.org/10.1002/2017GL073931>
- Becker, M.W., Ciervo, C., and Coleman, T., Laboratory testing of low frequency strain measured by distributed acoustic sensing, *SEG Technical Program Expanded Abstracts*, 2018, pp. 4963–4966.  
<https://doi.org/10.1190/segam2018-2997900.1>
- Bellefleur, G., Schetselaar, E., Wade, D., White, D., Enkin, R., and Schmitt, D.R., Vertical seismic profiling using distributed acoustic sensing with scatter-enhanced fibre-optic cable at the Cu–Au New Afton porphyry deposit, British Columbia, Canada, *Geophys. Prospect.*, 2020, vol. 68, pp. 313–333.  
<https://doi.org/10.1111/1365-2478.12828>



- Binder, G. and Chakraborty, D., Detecting microseismic events in downhole distributed acoustic sensing data using convolutional neural networks, *SEG Technical Program Expanded Abstracts*, 2019, pp. 4864–4868.  
<https://doi.org/10.1190/segam2019-3214863.1>
- Binder, G., Titov, A., Liu, Y., Simmons, J., Tura, A., Byerley, G., and Monk, D., Modeling the seismic response of individual hydraulic fracturing stages observed in a time-lapse distributed acoustic sensing vertical seismic profiling survey, *Geophysics*, 2020, vol. 85, no. 4, pp. T225–T235.  
<https://doi.org/10.1190/geo2019-0819.1>
- Booth, A.D., Christoffersen, P., Schoonman, C., Clarke, A., Hubbard, B., Law, R., Doyle, S.H., Chudley, T.R., and Chalari, A., Distributed acoustic sensing of seismic properties in a borehole drilled on a fast-flowing greenlandic outlet glacier, *Geophys. Res. Lett.*, 2020, vol. 47, no. 13, p. e2020GL088148.  
<https://doi.org/10.1029/2020GL088148>
- Borodin, I. and Segal, A., Real-time hydraulic fracture monitoring and wellbore characterization with distributed acoustic sensing of pumping noise, *Leading Edge*, 2020, vol. 39, no. 11, pp. 785–792.  
<https://doi.org/10.1190/tle39110785.1>
- Buimistryuk, G.Ya., *Informatsionno-izmeritel'naya tekhnika i tekhnologiya na osnove volokonno-opticheskikh datchikov i sistem* (Information-Measurement Technics and Technology Based on Fiber-Optic Sensors and Systems), St. Petersburg: IVA, GROTs Minatoma, 2005.
- Butov, O.V., Zotov, A.M., and Yatseev, V.A., Use of chirped pulse for recovering the phase of coherent reflectometer, *Foton-Ekspress*, 2019, no. 6, pp. 46–47.  
<https://doi.org/10.24411/2308-6920-2019-16018>
- Chambers, K., What is DAS and what is it measuring? <https://motionsignaltechnologies.com/what-is-das-and-what-is-it-measuring>. Cited January 12, 2022.
- Chang, T., Wang, Z., Yang, Y., Zhang, Y., Zheng, Z., Cheng, L., and Cui, H.-L., Fiber optic interferometric seismometer with phase feedback control, *Opt. Express*, 2020, vol. 28, pp. 6102–6122.  
<https://doi.org/10.1364/OE.385703>
- Chapeleau, X. and Bassil, A., A general solution to determine strain profile in the core of distributed fiber optic sensors under any arbitrary strain fields, *Sensors*, 2021, vol. 21, no. 16, p. 5423.  
<https://doi.org/10.3390/s21165423>
- Chen, D., Liu, Q., and He, Z., 108-km distributed acoustic sensor with 220-pε/√Hz strain resolution and 5-m spatial resolution, *J. Lightwave Technol.*, 2019, vol. 37, no. 18, pp. 4462–4468.  
<https://doi.org/10.1109/JLT.2019.2901276>
- Cheng, F., Chi, B., Lindsey, N.J., Dawe, T.C., and Ajo-Franklin, J.B., Utilizing distributed acoustic sensing and ocean bottom fiber optic cables for submarine structural characterization, *Sci. Rep.*, 2021, vol. 11, p. 5613.  
<https://doi.org/10.1038/s41598-021-84845-y>
- Correa, J., Pevzner, R., Bona, A., Tertyshnikov, K., Freifeld, B., Robertson, M., and Daley, T., 3D vertical seismic profile acquired with distributed acoustic sensing on tubing installation: A case study from the CO2CRC Otway project, *Interpretation*, 2019, vol. 7, no. 1, pp. SA11–SA19.  
<https://doi.org/10.1190/INT-2018-0086.1>
- Coscetta, A., Minardo, A., and Zeni, L., Distributed dynamic strain sensing based on Brillouin scattering in optical fibers, *Sensors*, 2020, vol. 20, no. 19, p. 5629.  
<https://doi.org/10.3390/s20195629>
- Currenti, G., Jousset, P., Chalari, A., Zuccarello, L., Napoli, R., Reinsch, T., and Krawczyk, C., Fibre optic distributed acoustic sensing of volcanic events at mt etna, *EGU General Assembly*, 2020, p. EGU2020-11461.  
<https://doi.org/10.5194/egusphere-egu2020-11641>
- Daley, T.M., Freifeld, B.M., Ajo-Franklin, J., Dou, S., Pevzner, R., Shulakova, V., Kashikar, S., Miller, D.E., Goetz, J., Hennings, J., and Lueth, S., Field testing of fiber-optic distributed acoustic sensing (DAS) for subsurface seismic monitoring, *Leading Edge*, 2013, vol. 32, no. 6, pp. 699–706.  
<https://doi.org/10.1190/tle32060699.1>
- Daley, T.M., Miller, D.E., Dodds, K., Cook, P., and Freifeld, B.M., Field testing of modular borehole monitoring with simultaneous distributed acoustic sensing and geophone vertical seismic profiles at Citronelle, Alabama, *Geophys. Prospect.*, 2016, vol. 64, no. 5, pp. 1318–1334.  
<https://doi.org/10.1111/1365-2478.12324>
- Dashkov, M.V. and Smirnov, A.S., Polarization reflectometry of optical fibers: Physical foundations, methods and applications (review article), *Prikl. Fotonika*, 2018, vol. 5, nos. 1–2, pp. 62–91.
- Dean, T., Cuny, T., and Hartog, A.H., The effect of gauge length on axially incident P-waves measured using fibre optic distributed vibration sensing, *Geophys. Prospect.*, 2017, vol. 65, no. 1, pp. 184–193.  
<https://doi.org/10.1111/1365-2478.12419>
- Denisov, A., Soto, M., and Thévenaz, L., Going beyond 1000000 resolved points in a Brillouin distributed fiber sensor: theoretical analysis and experimental demonstration, *Light Sci. Appl.*, 2016, vol. 5, p. e16074.  
<https://doi.org/10.1038/lsa.2016.74>
- Distributed Acoustic Sensing in Geophysics: Methods and Applications*, Li, M., Karrenbach, J., and Ajo-Franklin, J., Eds., John Wiley & Sons, 2021.
- Distributed fiber-optic sensors. Special systems. Photonics. <https://sphotronics.ru/catalog/fiber-sensing/>. Cited January 10, 2022.
- Distributed fiber sensors. Special systems. Photonics. <https://sphotronics.ru/solutions/raspredelennye-volokonnye-datchiki/>. Cited December 21, 2021.
- Dong, B., Tribaldos, V.R., Xing, X., Byna, S., Ajo-Franklin, J.B., and Wu, K., DASSA: Parallel DAS data storage and analysis for subsurface event detection, *IEEE Int. Parallel and Processing Symp. (IPDPS)*, 2020, pp. 254–263.  
<https://doi.org/10.1109/IPDPS47924.2020.00035>
- Dou, S., Lindsey, N., Wagner, A.M., Daley, T.M., Freifeld, B., Robertson, M., Peterson, J., Ulrich, C., Martin, E.R., and Ajo-Franklin, J.B., Distributed acoustic sensing for seismic monitoring of the near surface: A traffic-noise interferometry case study, *Sci. Rep.*, 2017, vol. 7, no. 1, p. 11620.  
<https://doi.org/10.1038/s41598-017-11986-4>
- Fang, G., Li, Y.E., Zhao, Y., and Martin, E.R., Urban near-surface seismic monitoring using distributed acoustic sensing, *Geophys. Res. Lett.*, 2020, vol. 47, no. 6, p. e2019GL086115.  
<https://doi.org/10.1029/2019GL086115>

- Faucher, F., de Hoop, M.V., and Scherzer, O., Reciprocity-gap misfit functional for distributed acoustic sensing, combining data from passive and active sources, *Geophysics*, 2021, vol. 86, no. 2, pp. R211–R220.  
<https://doi.org/10.1190/geo2020-0305.1>
- Fedorov, A.K., Anufriev, M.N., Zhirnov, A.A., Stepanov, K.V., Nesterov, E.T., Namiot, D.E., Karasik, V., and Pnev, A., Note: gaussian mixture model for event recognition in optical time-domain reflectometry based sensing systems, *Rev. Sci. Instrum.*, 2016, vol. 87, no. 3, p. 036017.  
<https://doi.org/10.1063/1.4944417>
- Fenta, M.C., Potter, D.K., and Szanyi, J., Fibre optic methods of prospecting: a comprehensive and modern branch of geophysics, *Surv. Geophys.*, 2021, vol. 42, pp. 551–584.  
<https://doi.org/10.1007/s10712-021-09634-8>
- Fernandez, I., Berrocal, C.G., and Rempling, R., Long-term performance of distributed optical fiber sensors embedded in reinforced concrete beams under sustained deflection and cyclic loading, *Sensors*, 2021, vol. 21, no. 19, p. 6338.  
<https://doi.org/10.3390/s21196338>
- Fernandez-Ruiz, M.R., Martins, H.F., Pastor-Graells, J., Martin-Lopez, S., and Gonzalez-Herraez, M., Phase-sensitive OTDR probe pulse shapes robust against modulation-instability fading, *Opt. Lett.*, 2016, vol. 41, no. 24, pp. 5756–5759.  
<https://doi.org/10.1364/OL.41.005756>
- Fernandez-Ruiz, M.R., Soto, M.A., Williams, E.F., Martin-Lopez, S., Zhan, Z., Gonzalez-Herraez, M., and Martins, H., Distributed acoustic sensing for seismic activity monitoring, *APL Photonics*, 2020, vol. 5, p. 030901.  
<https://doi.org/10.1063/1.5139602>
- Fiber-optic sensors of distribution of strain and temperature sensors (DSTS). [https://www.ozoptics.com/ALL-NEW\\_PDF/DTS0115RU.pdf](https://www.ozoptics.com/ALL-NEW_PDF/DTS0115RU.pdf). Cited January 10, 2022.
- Foster, S., Thermal noise limits for optical time domain reflectometry, *J. Lightwave Technol.*, 2021, vol. 39, no. 8, pp. 2514–2521.  
<https://doi.org/10.1109/JLT.2021.3052192>
- Fu, Y., Wang, Z., Zhu, R., Xue, N., Jiang, J., Lu, C., Zhang, B., Yang, L., Atubga, D., and Rao, Y., Ultra-long-distance hybrid BOTDA/ $\Phi$ -OTDR, *Sensors*, 2018, vol. 18, no. 4, p. 976.  
<https://doi.org/10.3390/s18040976>
- Gabai, H. and Eyal, A., On the sensitivity of distributed acoustic sensing, *Opt. Lett.*, 2016, vol. 41, no. 24, pp. 5648–5651.  
<https://doi.org/10.1364/OL.41.005648>
- Gabai, H., Botsev, Y., Hahami, M., and Eyal, A., Optical frequency domain reflectometry at maximum update rate using i/q detection, *Opt. Lett.*, 2015, vol. 40, no. 8, pp. 1725–1728.  
<https://doi.org/10.1364/OL.40.001725>
- Galkovski, T., Lemcherreq, Y., Mata-Falcon, J., and Kaufmann, W., Fundamental studies on the use of distributed fibre optical sensing on concrete and reinforcing bars, *Sensors*, 2021, vol. 21, no. 22, p. 7643.  
<https://doi.org/10.3390/s21227643>
- Gorshkov, B.G. and Taranov, M.A., Simultaneous optical fibre strain and temperature measurements in a hybrid distributed sensor based on Rayleigh and Raman scattering, *Quantum Electron.*, 2018, vol. 48, no. 2, pp. 184–187.  
<https://doi.org/10.1070/QEL16541>
- Gorshkov, B.G., Gorshkov, G.B., and Taranov, M.A., Simultaneous temperature and strain sensing using distributed raman optical time-domain reflectometry, *Laser Phys. Lett.*, 2017, vol. 14, no. 1, p. 015103.  
<https://doi.org/10.1088/1612-202X/14/1/015103>
- Gutscher, M.-A., Royer, J.-Y., Graindorge, D., Murphy, S., Klingelhoefer, F., Aiken, C., Cattaneo, A., Barreca, G., Quetel, L., Riccobene, G., Aurnia, S., Petersen, F., Lange, D., Urlaub, M., Krastel, S., Gross, F., Kopp, H., Moretti, M., Beranzoli, L., Lo Bue, N., and the FOCUS team, The FOCUS experiment 2020 (fiber optic cable use for seafloor studies of earthquake hazard and deformation), *EGU General Assembly*, 2020, p. EGU2020-5369.  
<https://doi.org/10.5194/egusphere-egu2020-5369>
- Han, B., Guan, H., Yao, J., Rao, Y.-J., Ran, Z., Gong, Y., Li, Q., Li, M., Zhang, R., An, S., Yu, G., and Wang, X., Distributed acoustic sensing with sensitivity-enhanced optical cable, *IEEE Sensors J.*, 2021, vol. 21, no. 4, pp. 4644–4651.  
<https://doi.org/10.1109/JSEN.2020.3035002>
- Hartog, A.H., Distributed sensors in the oil and gas industry, *Optical Fibre Sensors: Fundamentals for Development of Optimized Devices*, Villar, I. and Matias, I.R., Eds., pp. 151–191.  
<https://doi.org/10.1002/9781119534730.ch6>
- He, H., Yan, L., Qian, H., Zhang, X., Luo, B., and Pan, W., Enhanced range of the dynamic strain measurement in phase-sensitive OTDR with tunable sensitivity, *Opt. Express*, 2020a, vol. 28, no. 1, pp. 226–237.  
<https://doi.org/10.1364/OE.378257>
- He, X., Xu, X., Zhang, M., Xie, S., Liu, F., Gu, L., Zhang, Y., Yang, Y., and Lu, H., On the phase fading effect in the dual-pulse heterodyne demodulated distributed acoustic sensing system, *Opt. Express*, 2020b, vol. 28, no. 22, pp. 33433–33447.  
<https://doi.org/10.1364/OE.403263>
- Henninges, J., Martuganova, E., Stiller, M., Norden, B., and Krawczyk, C. Vertical seismic profiling with distributed acoustic sensing images the Rotliegend geothermal reservoir in the North German Basin down to 4.2 km depth, *Solid Earth*, 2020.  
<https://doi.org/10.5194/se-2020-169>
- Hong, C.-Y., Zhang, Y.-F., Zhang, M.-X., Ming, L., Leung, G., and Liu, L.-Q., Application of FBG sensors for geotechnical health monitoring, a review of sensor design, implementation methods and packaging techniques, *Sens. Actuators, A*, 2016, vol. 244, pp. 184–197.  
<https://doi.org/10.1016/j.sna.2016.04.033>
- Hornman, J.C., Field trial of seismic recording using distributed acoustic sensing with broadside sensitive fibre-optic cables, *Geophys. Prospect.*, 2017, vol. 65, pp. 35–46.  
<https://doi.org/10.1111/1365-2478.12358>
- Howe, B.M., Arbic, B.K., Aucan, J., Barnes, C.R., Bayliff, N., Becker, N., Butler, R., Doyle, L., Elipot, S., Johnson, G.C., Landerer, F., Lentz, S., Luther, D.S., Muller, M., Mariano, J., Panayotou, K., Rowe, C., Ota, H., Song, Y.T., Thomas, M., Thomas, P.N., Thompson, P., Tilmann, F., Weber, T., and Weinstein, S., Smart cables for observing the global ocean: Science and imple-

- mentation, *Front. Mar. Sci.*, 2019, vol. 6, p. 424.  
<https://doi.org/10.3389/fmars.2019.00424>
- Hudson, T.S., Baird, A.F., Kendall, J.M., Kufner, S.K., Brisbourne, A.M., Smith, A.M., Butcher, A., Chalari, A., and Clarke, A., Distributed acoustic sensing (DAS) for natural microseismicity studies: A case study from Antarctica, *J. Geophys. Res.: Solid Earth*, 2021, vol. 126, no. 7, p. e2020JB021493.  
<https://doi.org/10.1029/2020JB021493>
- Huff, O., Lellouch, A., Luo, B., Jin, G., and Biondi, B., Validating the origin of microseismic events in target reservoir using guided waves recorded by DAS, *Leading Edge*, 2020, vol. 39, no. 11, pp. 776–784.  
<https://doi.org/10.1190/tle39110776.1>
- Hull, R., Meek, R., Bello, H., Woller, K., and Wagner, J., Monitoring horizontal well hydraulic stimulations and geo-mechanical deformation processes in the unconventional shales of the midland basin using fiber-based time-lapse VSPs, microseismic, and strain data, *Leading Edge*, 2019, vol. 38, no. 2, pp. 130–137.  
<https://doi.org/10.1190/tle38021031.1>
- Huot, F. and Biondi, B., Machine learning algorithms for automated seismic ambient noise processing applied to das acquisition, *SEG Technical Program Expanded Abstracts*, 2018, pp. 5501–5505.  
<https://doi.org/10.1190/segam2018-w20-03.1>
- Ichikawa, M., Uchida, S., Katou, M., Kurosawa, I., Tamura, K., Kato, A., Ito, Y., De Groot, M., and Hara, S., Case study of hydraulic fracture monitoring using multiwell integrated analysis based on low-frequency DAS data, *Leading Edge*, 2020, vol. 39, no. 11, pp. 794–800.  
<https://doi.org/10.1190/tle39110794.1>
- Ide, S., Araki, E., and Matsumoto, H., Very broadband strain-rate measurements along a submarine fiber-optic cable off Cape Muroto, Nankai subduction zone, Japan, *Earth, Planets Space*, 2021, vol. 73, p. 63.  
<https://doi.org/10.1186/s40623-021-01385-5>
- Iida, D., Honda, N., and Oshida, H., Advances in distributed vibration sensing for optical communication fiber state visualization, *Opt. Fiber Tech.*, 2020, vol. 57, p. 102263.  
<https://doi.org/10.1016/j.yofte.2020.102263>
- Ilinskiy, D.A., Alekseev, A.E., Ganzha, O.Yu., Semikin, D.E., and Ojha, M., Use of fiber optic communication lines with a phase-sensitive reflectometer for recording seismic signals, *Seism. Instrum.*, 2021, vol. 57, pp. 231–248.  
<https://doi.org/10.3103/S0747923921030051>
- Ivanov, V., Longoni, L., Ferrario, M., Brunero, M., Arosio, D., and Papini, M., Applicability of an interferometric optical fibre sensor for shallow landslide monitoring—Experimental tests, *Eng. Geol.*, 2021, vol. 288, p. 106128.  
<https://doi.org/10.1016/j.enggeo.2021.106128>
- Jestin, C., Hibert, C., Calbris, G., and Lanticq, V., Integration of machine learning on distributed acoustic sensing surveys, *EGU General Assembly*, 2020, pp. EGU2020–7495.  
<https://doi.org/10.5194/egusphere-egu2020-7495>
- Jia, H., Liang, S., Lou, S., and Sheng, X., A  $k$ -nearest neighbor algorithm-based near category support vector machine method for event identification of  $\varphi$ -OTDR, *IEEE Sens. J.*, 2019, vol. 19, no. 10, pp. 3683–3689.  
<https://doi.org/10.1109/JSEN.2019.2891750>
- Jousset, P., Reinsch, T., Ryberg, T., Blanck, H., Clarke, A., Aghayev, R., Hersir, G.P., Hennings, J., Weber, M., and Krawczyk, C.M., Dynamic strain determination using fibre-optic cables allows imaging of seismological and structural features, *Nat. Commun.*, 2018, vol. 9, no. 1, p. 2509.  
<https://doi.org/10.1038/s41467-018-04860-y>
- Kapa, T., Schreier, A., and Krebber, K., A 100-km BOFDA assisted by first-order bi-directional Raman amplification, *Sensors*, 2019, vol. 19, no. 7, p. 1527.  
<https://doi.org/10.3390/s19071527>
- Keul, P.R., Mastin, E., Blanco, J., Maguerez, M., Bostick, T., and Knudsen, S., Using a fiber-optic seismic array for well monitoring, *Leading Edge*, 2005, vol. 24, no. 1, pp. 68–70.  
<https://doi.org/10.1190/1.1859704>
- Kishida, K., Guzik, A., Nishiguchi, K., Li, C.-H., Azuma, D., Liu, Q., and He, Z., Development of real-time time gated digital (TGD) OFDR method and its performance verification, *Sensors*, 2021, vol. 21, no. 14, p. 4865.  
<https://doi.org/10.3390/s21144865>
- Kislov, K.V. and Gravirov, V.V., Some remarks on the seismometric experiments taking into account the thickness of the frozen layer soil, *Problems of Geocosmos-2018*, Yanovskaya, T., Kosterov, A., Bobrov, N., Divin, A., Sar-aev, A., and Zolotova, N., Eds., Springer Proceedings in Earth and Environmental Sciences, Cham: Springer, 2018, pp. 263–269.  
[https://doi.org/10.1007/978-3-030-21788-4\\_22](https://doi.org/10.1007/978-3-030-21788-4_22)
- Kislov, K.V. and Gravirov, V.V., Rotational seismology: Review of achievements and outlooks, *Seism. Instrum.*, 2021, vol. 57, pp. 187–202.  
<https://doi.org/10.3103/S0747923921020262>
- Klaasen, S., Paitz, P., Lindner, N., Dettmer, J., and Fichtner, A., Distributed acoustic sensing in volcano-glacial environments—Mount Meager, British Columbia, *J. Geophys. Res.: Solid Earth*, 2021, vol. 126, no. 11, p. e2021JB022358.  
<https://doi.org/10.1029/2021JB022358>
- Klaasen, S., Thrastarson, S., Fichtner, A., Çubuk-Sabuncu, Y., and Jónsdóttir, K., Sensing Iceland’s most active volcano with a “buried hair”, *EOS*, 2022, p. 103.  
<https://doi.org/10.1029/2022EO220007>
- Kobayashi, Y., Uematsu, Y., Mochiji, S., and Xue, Z., A field experiment of walkaway distributed acoustic sensing vertical seismic profile in a deep and deviated onshore well in Japan using a fibre optic cable deployed inside coiled tubing, *Geophys. Prospect.*, 2020, vol. 68, pp. 501–520.  
<https://doi.org/10.1111/1365-2478.12863>
- Krebber, K., Smart technical textiles based on fiber optic sensors, *Current Developments in Optical Fiber Technology*, Harun, S.W. and Arof, H., Eds., London: IntechOpen, 2013.  
<https://doi.org/10.5772/54244>
- Kuvshinov, B., Interaction of helically wound fibre-optic cables with plane seismic waves, *Geophys. Prospect.*, 2016, vol. 64, no. 3, pp. 671–688.  
<https://doi.org/10.1111/1365-2478.12303>
- Kye, M., Lee, S.-M., Choi, K.-M., Lee, Y., and Park, K.-Y., A surveillance system of fiber-optic cables with multi-channel DAS and CNN, *IEEE Photonics Technol. Lett.*, 2021, vol. 33, no. 15, pp. 753–756.  
<https://doi.org/10.1109/LPT.2021.3091145>

- Lellouch, A. and Biondi, B.L., Seismic applications of downhole das, *Sensors*, 2021, vol. 21, no. 9, p. 2897. <https://doi.org/10.3390/s21092897>
- Lellouch, A., Meadows, M.A., Nemeth, T., and Biondi, B., Fracture properties estimation using distributed acoustic sensing recording of guided waves in unconventional reservoirs, *Geophysics*, 2020, vol. 85, no. 5, pp. M85–M95. <https://doi.org/10.1190/geo2019-0793.1>
- Lellouch, A., Biondi, E., Biondi, B.L., Luo, B., Jin, G., and Meadows, M.A., Properties of a deep seismic waveguide measured with an optical fiber, *Phys. Rev. Res.*, 2021a, vol. 3, p. 013164. <https://doi.org/10.1103/PhysRevResearch.3.013164>
- Lellouch, A., Schultz, R., Lindsey, N.J., Biondi, B.L., and Ellsworth, W.L., Low-magnitude seismicity with a downhole distributed acoustic sensing array - examples from the forge geothermal experiment, *J. Geophys. Res.: Solid Earth*, 2021b, vol. 126, no. 1, p. e2020JB020462. <https://doi.org/10.1029/2020JB020462>
- Li, Z. and Zhan, Z., Pushing the limit of earthquake detection with distributed acoustic sensing and template matching: a case study at the brady geothermal field, *Geophys. J. Int.*, 2018, vol. 215, no. 3, pp. 1583–1593. <https://doi.org/10.1093/gji/ggy359>
- Li, Z., Shen, Z., Yang, Y., Williams, E., Wang, X., and Zhan, Z., Rapid response to the 2019 Ridgecrest earthquake with distributed acoustic sensing, *AGU Adv.*, 2021, vol. 2, no. 2, p. e2021AV000395. <https://doi.org/10.1029/2021AV000395>
- Liang, J., Wang, Z., Lu, B., Wang, X., Li, L., Ye, Q., Qu, R., and Cai, H., Distributed acoustic sensing for 2D and 3D acoustic source localization, *Opt. Lett.*, 2019, vol. 44, pp. 1690–1693. <https://doi.org/10.1364/OL.44.001690>
- Lindsey, N.J. and Martin, E.R., Fiber-optic seismology, *Ann. Rev. Earth Planet. Sci.*, 2021, vol. 49, no. 1, pp. 309–336. <https://doi.org/10.1146/annurev-earth-072420-065213>
- Lindsey, N.J., Martin, E.R., Dreger, D.S., Freifeld, B., Cole, S., James, S.R., Biondi, B.L., and Ajo-Franklin, J.B., Fiber-optic network observations of earthquake wavefields, *Geophys. Res. Lett.*, 2017, vol. 44, no. 23, pp. 11792–11799. <https://doi.org/10.1002/2017GL075722>
- Lindsey, N.J., Rademacher, H., and Ajo-Franklin, J.B., On the broadband instrument response of fiber-optic das arrays, *J. Geophys. Res.: Solid Earth*, 2020, vol. 125, no. 2, p. e2019JB018145. <https://doi.org/10.1029/2019JB018145>
- Liokumovich, L.B., Ushakov, N.A., Kotov, O.I., Bisyarin, M.A., and Hartog, A.H., Fundamentals of optical fiber sensing schemes based on coherent optical time domain reflectometry: signal model under static fiber conditions, *J. Lightwave Technol.*, 2015, vol. 33, no. 17, pp. 3660–3671. <https://doi.org/10.1109/JLT.2015.2449085>
- Lior, I., Sladen, A., Rivet, D., Ampuero, J.-P., Hello, Y.M., Lamare, P., Jestin, C., Tsagkli, S., and Markou, C., On the detection capabilities of underwater distributed acoustic sensing, *J. Geophys. Res.: Solid Earth*, 2020, vol. 126, no. 3, p. e2020JB020925. <https://doi.org/10.1029/2020JB020925>
- Lior, I., Sladen, A., Mercerat, D., Ampuero, J.-P., Rivet, D., and Sambolian, S., Strain to ground motion conversion of distributed acoustic sensing data for earthquake magnitude and stress drop determination, *Solid Earth*, 2021a, vol. 12, pp. 1421–1442. <https://doi.org/10.5194/se-12-1421-2021>
- Lior, I., Sladen, A., Rivet, D., Ampuero, J.-P., Hello, Y., Becerril, C., Martins, H.F., Lamare, P., Jestin, C., Tsagkli, S., and Markou, C., On the detection capabilities of underwater distributed acoustic sensing, *J. Geophys. Res.: Solid Earth*, 2021b, vol. 126, no. 3, p. e2020JB020925. <https://doi.org/10.1029/2020JB020925>
- Liu, S.P., Shi, B., Gu, K., Zhang, C.-C., He, J.-H., Wu, J.-H., and Wei, G.-Q., Fiber-optic wireless sensor network using ultra-weak fiber Bragg gratings for vertical subsurface deformation monitoring, *Nat. Hazards*, 2021, vol. 109, pp. 2557–2573. <https://doi.org/10.1007/s11069-021-04932-1>
- Liu, Y., Jin, G., Wu, K., and Moridis, G., Hydraulic-fracture-width inversion using low-frequency distributed-acoustic-sensing strain data—Part I: Algorithm and sensitivity analysis, *SPE J.*, 2021a, vol. 26, no. 01, pp. 359–371. <https://doi.org/10.2118/204225-PA>
- Liu, Y., Wu, K., Jin, G., Moridis, G., Kerr, E., Scofield, R., and Johnson, A., Fracture-hit detection using LF-DAS signals measured during multifracture propagation in unconventional reservoirs, *SPE Reservoir Eval. Eng.*, 2021b, vol. 24, no. 03, pp. 523–535. <https://doi.org/10.2118/204457-PA>
- Liu, Y., Yang, J., Wu, B., Lu, B., Shuai, L., Wang, Z., Ye, L., Ying, K., Ye, Q., Qu, R., and Cai, H., High SNR  $\Phi$ -OTDR with multi-transverse modes heterodyne matched-filtering technology, *Sensors*, 2021c, vol. 21, no. 22, p. 7460. <https://doi.org/10.3390/s21227460>
- Lopez-Mercado, C.A., Korobko, D.A., Zolotovskii, I.O., and Fotiadi, A.A., Application of dual-frequency self-injection locked DFB laser for Brillouin optical time domain analysis, *Sensors*, 2021, vol. 21, no. 20, p. 6859. <https://doi.org/10.3390/s21206859>
- Lu, P., Lalam, N., Badar, M., Liu, B., Chorpeneing, B.T., Buric, M.P., and Ohodnicki, P.R., Distributed optical fiber sensing: review and perspective, *Appl. Phys. Rev.*, 2019, vol. 6, no. 4, p. 041302. <https://doi.org/10.1063/1.5113955>
- Lund, B., Stork, A., Roth, M., David, A., Clarke, A., Nygren, C., and Johansson, S., Comparing high-sensitivity geophones to fiber-optic DAS technologies in a hard-rock VSP survey, *EGU General Assembly*, 2020, p. EGU2020-18525. <https://doi.org/10.5194/egusphere-egu2020-18525>
- Luo, B., Trainor-Guitton, W., Bozdağ, E., LaFlame, L., Cole, S., and Karrenbach, M., Horizontally orthogonal distributed acoustic sensing array for earthquake- and ambient-noise-based multichannel analysis of surface waves, *Geophys. J. Int.*, 2020, vol. 222, no. 3, pp. 2147–2161. <https://doi.org/10.1093/gji/ggaa293>
- Luo, B., Jin, G., and Stanek, F., Near-field strain in distributed acoustic sensing-based microseismic observation, *Geophysics*, 2021, vol. 86, no. 5, pp. 49–60. <https://doi.org/10.1190/geo2021-0031.1>
- Lv, H., Zeng, X., Bao, F., Xie, J., Lin, R., Song, Z., and Zhang, G., ADE-Net: a deep neural network for das earthquake detection trained with a limited number of positive

- samples, *IEEE Trans. Geosci. Remote Sens.*, 2022, vol. 60, p. 5912111.  
<https://doi.org/10.1109/TGRS.2022.3143120>
- Marra, G., Clivati, C., Luckett, R., Tampellini, A., Kronjager, J., Wright, L., Mura, A., Levi, F., Robinson, S., Xuereb, A., Baptie, B., and Calonico, D., Ultrastable laser interferometry for earthquake detection with terrestrial and submarine cables, *Science*, 2018, vol. 361, no. 6401, pp. 486–490.  
<https://doi.org/10.1126/science.aat4458>
- Martins, H.F., Shi, K., Thomsen, B.C., Martin-Lopez, S., Gonzalez-Herraez, M., and Savory, S.J., Real time dynamic strain monitoring of optical links using the back reflection of live PSK data, *Opt. Express*, 2016, vol. 24, pp. 22303–22318.  
<https://doi.org/10.1364/OE.24.022303>
- Masoudi, A. and Newson, T.P., Contributed review: distributed optical fibre dynamic strain sensing, *Rev. Sci. Instrum.*, 2016, vol. 87, p. 011501.  
<https://doi.org/10.1063/1.4939482>
- Mateeva, A., Lopez, J., Chalenski, D., Tatanova, M., Zwartjes, P., Yang, Z., Bakku, S., de Vos, K., and Potters, H., 4D DAS VSP as a tool for frequent seismic monitoring in deep water, *Leading Edge*, 2017, vol. 36, pp. 995–1000.  
<https://doi.org/10.1190/tle36120995.1>
- Matias, L., Omar, Y., Carrilho, F., Sa, V., Omira, R., Corella, C., Perdigao, R.A.P., and Loureiro, A., The contribution of the CAM fibre optic submarine cable telecom ring to the early warning of tsunami and earthquakes, *EGU General Assembly*, 2020, p. EGU2020-13988.  
<https://doi.org/10.5194/egusphere-egu2020-13988>
- Matsumoto, H., Araki, E., Kimura, T., Fujie, G., Shiraishi, K., Tonegawa, T., Obana, K., Arai, R., Kaiho, Y., Nakamura, Y., Yokobiki, T., Kodaira, S., Takahashi, N., Ellwood, R., Yartsev, V., and Karrenbach, M., Detection of hydroacoustic signals on a fiber-optic submarine cable, *Sci. Rep.*, 2021, vol. 11, p. 2797.  
<https://doi.org/10.1038/s41598-021-82093-8>
- Meng, Z., Chen, W., Wang, J., Hu, X., Chen, M., and Zhang, Y., Recent progress in fiber-optic hydrophones, *Photonic Sens.*, 2021, vol. 11, pp. 109–122.  
<https://doi.org/10.1007/s13320-021-0618-5>
- Min, R., Liu, Z., Pereira, L., Yang, C., Sui, Q., and Marques, C., Optical fiber sensing for marine environment and marine structural health monitoring: a review, *Opt. Laser Technol.*, 2021, vol. 140, p. 107082.  
<https://doi.org/10.1016/j.optlastec.2021.107082>
- Minardo, A., Bernini, R., Ruiz-Lombera, R., Mirapeix, J., Lopez-Higuera, J.M., and Zeni, L., Proposal of Brillouin optical frequency-domain reflectometry (BOFDR), *Opt. Express*, 2016, vol. 24, pp. 29994–30001.  
<https://doi.org/10.1364/OE.24.029994>
- Minardo, A., Zeni, L., Coscetta, A., Catalano, E., Zeni, G., Damiano, E., De Cristofaro, M., and Olivares, L., Distributed optical fiber sensor applications in geotechnical monitoring, *Sensors*, 2021, vol. 21, no. 22, p. 7514.  
<https://doi.org/10.3390/s21227514>
- Mizuno, Y., Lee, H., and Nakamura, K., Recent advances in Brillouin optical correlation-domain reflectometry, *Appl. Sci.*, 2018, vol. 8, no. 10, p. 1845.  
<https://doi.org/10.3390/app8101845>
- Motil, A., Bergman, A., and Tur, M., State of the art of Brillouin fiber-optic distributed sensing, *Opt. Laser Technol.*, 2016, vol. 78, pp. 81–103.  
<https://doi.org/10.1016/j.optlastec.2015.09.013>
- Muanenda, Y., Recent advances in distributed acoustic sensing based on phase-sensitive optical time domain reflectometry, *J. Sens.*, 2018, vol. 2018, p. 3897873.  
<https://doi.org/10.1155/2018/3897873>
- Naldrett, G., Parker, T., Shatalin, S., and Mondanos, M., High-resolution carina distributed acoustic fibre-optic sensor for permanent reservoir monitoring and extending the reach into subsea fields, *First Break*, 2020, vol. 38, pp. 71–76.  
<https://doi.org/10.3997/1365-2397.fb2020012>
- Nayak, A., Ajo-Franklin, J., and The Imperial Valley Dark Fiber Team, Distributed acoustic sensing using dark fiber for array detection of regional earthquakes, *Seismol. Res. Lett.*, 2021a, vol. 92, no. 4, pp. 2441–2452.  
<https://doi.org/10.1785/0220200416>
- Nayak, A. and Ajo-Franklin, J., The imperial valley dark fiber team. measurement of surface-wave phase-velocity dispersion on mixed inertial seismometer—Distributed acoustic sensing seismic noise cross-correlations, *Bull. Seismol. Soc. Am.*, 2021b, vol. 111, no. 6, pp. 3432–3450.  
<https://doi.org/10.1785/0120210028>
- Ning, I.L.C. and Sava, P., High-resolution multi-component distributed acoustic sensing, *Geophys. Prospect.*, 2018a, vol. 66, pp. 1111–1122.  
<https://doi.org/10.1111/1365-2478.12634>
- Ning, I.L.C. and Sava, P., Multicomponent distributed acoustic sensing: concept and theory, *Geophysics*, 2018b, vol. 83, no. 2, pp. P1–P8.  
<https://doi.org/10.1190/geo2017-0327.1>
- Paitz, P., Edme, P., Gräff, D., Walter, F., Doetsch, J., Chalarí, A., Schmelzbach, C., and Fichtner, A., Empirical investigations of the instrument response for distributed acoustic sensing (DAS) across 17 octaves, *Bull. Seismol. Soc. Am.*, 2020, vol. 111, no. 1, pp. 1–10.  
<https://doi.org/10.1785/0120200185>
- Papp, B., Donno, D., Martin, J.E., and Hartog, A.H., A study of the geophysical response of distributed fibre optic acoustic sensors through laboratory-scale experiments, *Geophys. Prospect.*, 2017, vol. 65, pp. 1186–1204.  
<https://doi.org/10.1111/1365-2478.12471>
- Parker, L.M., Thurber, C.H., Zeng, X., Li, P., Lord, N.E., Fratta, D., Wang, H.F., Robertson, M.C., Thomas, A.M., Karplus, M.S., Nayak, A., and Feigl, K.L., Active-source seismic tomography at the Brady Geothermal Field, Nevada, with dense nodal and fiber-optic seismic arrays, *Seismol. Res. Lett.*, 2018, vol. 89, no. 5, pp. 1629–1640.  
<https://doi.org/10.1785/0220180085>
- Pastor-Graells, J., Martins, H.F., Garcia-Ruiz, A., Martin-Lopez, S., and Gonzalez-Herraez, M., Single-shot distributed temperature and strain tracking using direct detection phase-sensitive OTDR with chirped pulses, *Opt. Express*, 2016, vol. 24, pp. 13121–13133.  
<https://doi.org/10.1364/OE.24.013121>
- Peng, F. and Cao, X., A hybrid  $\Phi$ /B-OTDR for simultaneous vibration and strain measurement, *Photonic Sens.*, 2016, vol. 6, no. 2, pp. 121–126.  
<https://doi.org/10.1007/s13320-016-0289-9>

- Pevzner, R., Gurevich, B., Pirogova, A., Tertyshnikov, K., and Glubokovskikh, S., Repeat well logging using earthquake amplitudes measured by distributed acoustic sensors, *Leading Edge*, 2020, vol. 39, no. 7, pp. 513–517. <https://doi.org/10.1190/tle39070513.1>
- Popik, S., Pevzner, R., Bona, A., Tertyshnikov, K., Glubokovskikh, S., and Gurevich, B., Estimation of P-wave anisotropy parameters from 3D vertical seismic profile with distributed acoustic sensors and geophones for seismic imaging in the CO2CRC Otway Project, *Geophys. Prospect.*, 2021, vol. 69, pp. 842–855. <https://doi.org/10.1111/1365-2478.13080>
- Rajan, G., *Optical Fiber Sensors: Advanced Techniques and Applications*, Boca Raton, Fla.: CRC Press, 2017.
- Ramakrishnan, M., Rajan, G., Semenova, Y., Boczkowska, A., Domański, A., Wolinski, T., and Farrell, G., Measurement of thermal elongation induced strain of a composite material using a polarization maintaining photonic crystal fiber sensor, *Sens. Actuators, A*, 2013, vol. 190, pp. 44–51. <https://doi.org/10.1016/j.sna.2012.11.010>
- Rao, Y., Wang, Z., Wu, H., Ran, Z., and Han, B., Recent advances in phase-sensitive optical time domain reflectometry ( $\Phi$ -OTDR), *Photonic Sens.*, 2021, vol. 11, pp. 1–30. <https://doi.org/10.1007/s13320-021-0619-4>
- Reinsch, T., Thurley, T., and Jousset, P., On the mechanical coupling of a fiber optic cable used for distributed acoustic/vibration sensing applications—A theoretical consideration, *Meas. Sci. Technol.*, 2017, vol. 28, p. 127003. <https://doi.org/10.1088/1361-6501/aa8ba4>
- Reinsch, T., Jousset, P., and Krawczyk, C.M., Fiber optic distributed strain sensing for seismic applications, *Encyclopedia of Solid Earth Geophysics*, Gupta, H.K., Ed., Encyclopedia of Earth Sciences Series, Cham: Springer, 2020, pp. 1–5. [https://doi.org/10.1007/978-3-030-10475-7\\_284-1](https://doi.org/10.1007/978-3-030-10475-7_284-1)
- Rohwetter, P., Eisermann, R., and Krebber, K., Random quadrature demodulation for direct detection single-pulse Rayleigh C-OTDR, *J. Lightwave Technol.*, 2016, vol. 34, no. 19, pp. 4437–4444. <https://doi.org/10.1109/JLT.2016.2557586>
- Sheng, L., Yan, J., Li, L., Yuan, M., Zhou, S., Xu, R., Liu, J., Nian, F., Li, L., and Liu, Z., Distributed temperature sensing system based on Brillouin scattering effect using a single-photon detector, *Int. J. Opt.*, 2021, vol. 2021, p. 6623987. <https://doi.org/10.1155/2021/6623987>
- Shi, Y., Wang, Y., Zhao, L., and Fan, Z., An event recognition method for  $\Phi$ -OTDR sensing system based on deep learning, *Sensors*, 2019, vol. 19, no. 15, p. 3421. <https://doi.org/10.3390/s19153421>
- Shinohara, M., Yamada, T., Akuhara, T., Mochizuki, K., and Sakai, S., Precise distributed acoustic sensing measurements by using seafloor optical fiber cable system for seismic monitoring, *EGU General Assembly*, 2020, p. EGU2020-12055. <https://doi.org/10.5194/egusphere-egu2020-12055>
- Shragge, J., Yang, J., Issa, N., Roelens, M., Dentith, M., and Schediwy, S., Low-frequency ambient distributed acoustic sensing (DAS): Case study from Perth, Australia, *Geophys. J. Int.*, 2021, vol. 226, no. 1, pp. 564–581. <https://doi.org/10.1093/gji/ggab111>
- Shuvalov, A.A., Pnev, A.B., Ignat'ev, V.I., Zhirnov, A.A., Oshkin, A.N., Nesterov, E.T., Stepanov, K.V., Tarasov, A.V., Kon'kov, A.I., and Chernutskii, A.O., Possibility of using distributed acoustic probing for solving geophysical problems, in *14-ya ezhegodnaya nauchno-prakticheskaya konferentsiya i vystavka Inzhenernaya i rudnaya geofizika 2018. 23–27 aprelya 2018* (14th Annular Sci.-Pract. Conf. and Exhibition Engineering and Mining Geophysics), Almaty: EAGE, 2018a. <https://doi.org/10.3997/2214-4609.201800591>
- Shuvalov, A.A., Pnev, A.B., Ignatev, V.I., Zhirnov, A.A., Chernutsky, A.O., and Nesterov, E.T., Possibility of distributed acoustic sensing (DAS) for geophysical problems solution, *Conf. Proc., Engineering and Mining Geophysics*, 2018, European Association of Geoscientists & Engineers, 2018b, pp. 1–7. <https://doi.org/10.3997/2214-4609.201800591>
- Sladen, A., Rive, D., Ampuero, J.P., De Barros, L., Hello, Y., Calbris, G., and Lamare, P., Distributed sensing of earthquakes and ocean-solid earth interactions on seafloor telecom cables, *Nat. Commun.*, 2019, vol. 10, p. 5777. <https://doi.org/10.1038/s41467-019-13793-z>
- Smolinski, K., Paitz, P., Bowden, D., Edme, P., Kugler, F., and Fichtner, A., Urban distributed acoustic sensing using in-situ fibre beneath Bern, Switzerland, *EGU General Assembly*, 2020, pp. EGU2020-8225. <https://doi.org/10.5194/egusphere-egu2020-8225>
- Song, Z., Zeng, X., and Thurber, C.H., Surface-wave dispersion spectrum inversion method applied to Love and Rayleigh waves recorded by distributed acoustic sensing, *Geophysics*, 2021a, vol. 86, no. 1, pp. EN1–EN12. <https://doi.org/10.1190/geo2019-0691.1>
- Song, Z., Zeng, X., Xie, J., Bao, F., and Zhang, G., Sensing shallow structure and traffic noise with fiber-optic internet cables in an urban area, *Surv. Geophys.*, 2021b, vol. 42, pp. 1401–1423. <https://doi.org/10.1007/s10712-021-09678-w>
- Soriano-Amat, M., Martins, H.F., Durán, V., Costa, L., Martín-López, S., Gonzalez-Herreraez, M., and Fernández-Ruiz, M.R., Time-expanded phase-sensitive optical time-domain reflectometry, *Light Sci. Appl.*, 2021, vol. 10, p. 51. <https://doi.org/10.1038/s41377-021-00490-0>
- Spica, Z.J., Nishida, K., Akuhara, T., Pétréris, F., Shinohara, M., and Yamada, T., Marine sediment characterized by ocean-bottom fiber-optic seismology, *Geophys. Rev. Lett.*, 2020a, vol. 47, no. 16, p. e2020GL088360. <https://doi.org/10.1029/2020GL088360>
- Spica, Z.J., Perton, M., Martin, E.R., Beroza, G.C., and Biondi, B., Urban seismic site characterization by fiber-optic seismology, *J. Geophys. Res.: Solid Earth*, 2020b, vol. 125, p. e2019JB018656. <https://doi.org/10.1029/2019JB018656>
- Stork, A.L., Baird, A.F., Horne, S.A., Naldrett, G., Lapsin, S., Kendall, J.-M., Wookey, J., Verdon, J.P., Clarke, A., and Williams, A., Application of machine learning to microseismic event detection in distributed acoustic sensing data, *Geophysics*, 2020, vol. 85, no. 5, pp. KS149–KS160. <https://doi.org/10.1190/geo2019-0774.1>
- Tangudu, R. and Sahu, P.K., Strain resolution and spatial resolution improvement of BOCDR-based DSS system using particle swarm optimization algorithm, *Optical and Wireless Technologies*, Janyani, V., Singh, G., Tiwari, M.,

- and d'Alessandro, A., Eds., Lecture Notes in Electrical Engineering, vol. 546, Singapore: Springer, 2019, pp. 179–192.  
[https://doi.org/10.1007/978-981-13-6159-3\\_20](https://doi.org/10.1007/978-981-13-6159-3_20)
- Taweentananon, K., Landrø, M., Brenne, J.K., and Haukanes, A., Distributed acoustic sensing for near-surface imaging using submarine telecommunication cable: a case study in the Trondheimsfjord, Norway, *Geophysics*, 2021, vol. 86, no. 5, pp. B303–B320.  
<https://doi.org/10.1190/geo2020-0834.1>
- Titov, A., Binder, G., Liu, Y., Jin, G., Simmons, J., Tura, A., Monk, D., Byerley, G., and Yates, M., Modeling and interpretation of scattered waves in interstage distributed acoustic sensing vertical seismic profiling survey, *Geophysics*, 2021, vol. 86, no. 2, pp. D93–D102.  
<https://doi.org/10.1190/geo2020-0293.1>
- Tkachenko, A.Yu., Lobach, I.A., and Kablukov, S.I., Optical frequency reflectometer based on self-scanning fiber laser, *Foton-Ekspress*, 2019, no. 6, pp. 44–45.  
<https://doi.org/10.24411/2308-6920-2019-16017>
- Tribaldos, V.R. and Ajo-Franklin, J.B., Aquifer monitoring using ambient seismic noise recorded with distributed acoustic sensing (DAS) deployed on dark fiber, *J. Geophys. Res.: Solid Earth*, 2021, vol. 126, no. 4, p. e2020JB021004.  
<https://doi.org/10.1029/2020JB021004>
- Van den Ende, M.P.A. and Ampuero, J.-P., Evaluating seismic beamforming capabilities of distributed acoustic sensing arrays, *Solid Earth*, 2021, vol. 12, pp. 915–934.  
<https://doi.org/10.5194/se-12-915-2021>
- Van Putten, L.D., Masoudi, A., Snook, J., and Brambilla, G., Numerical modelling of a distributed acoustic sensor based on ultra-low loss-enhanced backscattering fibers, *Sensors*, 2021, vol. 21, no. 20, p. 6869.  
<https://doi.org/10.3390/s21206869>
- Verdon, J.P., Horne, S.A., Clarke, A., Stork, A.L., Baird, A.F., and Kendall, J.-M., Microseismic monitoring using a fiber-optic distributed acoustic sensor array, *Geophysics*, 2020, vol. 85, no. 3, pp. KS89–KS99.  
<https://doi.org/10.1190/geo2019-0752.1>
- Volokonno-opticheskaya tekhnika: istoriya, dostizheniya, perspektivy* (Fiber-Optic Technology: History, Achievements, and Outlooks), Dmitriev, S.A. and Slepov, N.N., Eds., Moscow: Connect, 2000.
- Wagner, A.M., Lindsey, N.J., Dou, S., Gelvin, A., Saari, S., Williams, C., Ekblaw, I., Ulrich, C., Borglin, S., Morales, A., and Ajo-Franklin, J., Permafrost degradation and subsidence observations during a controlled warming experiment, *Sci. Rep.*, 2018, vol. 8, p. 10908.  
<https://doi.org/10.1038/s41598-018-29292-y>
- Walter, F., Gräff, D., Lindner, F., Paitz, P., Köpfl, M., Chmiel, M., and Fichtner, A., Distributed acoustic sensing of microseismic sources and wave propagation in glaciated terrain, *Nat. Commun.*, 2020, vol. 11, p. 2436.  
<https://doi.org/10.1038/s41467-020-15824-6>
- Wamriew, D., Pevzner, R., Maltsev, E., and Pissarenko, D., Deep neural networks for detection and location of microseismic events and velocity model inversion from microseismic data acquired by distributed acoustic sensing array, *Sensors*, 2021, vol. 21, no. 19, p. 6627.  
<https://doi.org/10.3390/s21196627>
- Wang, H.F., Zeng, X., Miller, D.E., Fratta, D., Feigl, K.L., Thurber, C.H., and Mellors, R.J., Ground motion response to an  $M_L$  4.3 earthquake using co-located distributed acoustic sensing and seismometer arrays, *Geophys. J. Int.*, 2018, vol. 213, no. 3, pp. 2020–2036.  
<https://doi.org/10.1093/gji/ggy102>
- Wang, Z.N., Zeng, J.J., Li, J., Fan, M.Q., Wu, H., Peng, F., Zhang, L., Zhou, Y., and Rao, Y.J., Ultra-long phase-sensitive OTDR with hybrid distributed amplification, *Opt. Lett.*, 2014, vol. 39, pp. 5866–5869.  
<https://doi.org/10.1364/OL.39.005866>
- Wang, Z., Zheng, H., Li, L., Liang, J., Wang, X., Lu, B., Ye, Q., Qu, R., and Cai, H., Practical multi-class event classification approach for distributed vibration sensing using deep dual path network, *Opt. Express*, 2019, vol. 27, pp. 23682–23692.  
<https://doi.org/10.1364/OE.27.023682>
- Wang, Z., Lu, B., Ye, Q., and Cai, H., Recent progress in distributed fiber acoustic sensing with  $\Phi$ -OTDR, *Sensors*, 2020, vol. 20, no. 22, p. 6594.  
<https://doi.org/10.3390/s20226594>
- Wu, H., Yang, M., Yang, S., Lu, H., Wang, C., and Rao, Y., A novel DAS signal recognition method based on spatiotemporal information extraction with 1DCNNs-BiLSTM network, *IEEE Access*, 2020, vol. 8, pp. 119448–119457.  
<https://doi.org/10.1109/ACCESS.2020.3004207>
- Wu, Y., Richter, P., Hull, R., and Farhadiroushan, M., Hydraulic frac-hit corridor (FHC) monitoring and analysis with high-resolution distributed acoustic sensing (DAS) and far-field strain (FFS) measurements, *First Break*, 2020, vol. 38, pp. 65–70.  
<https://doi.org/10.3997/1365-2397.fb2020045>
- Wuestefeld, A. and Weinzierl, W., Design considerations for using distributed acoustic sensing for cross-well seismics: A case study for CO<sub>2</sub> storage, *Geophys. Prospect.*, 2020, vol. 68, pp. 1893–1905.  
<https://doi.org/10.1111/1365-2478.12965>
- Xiong, J., Wang, Z., Wu, Y., and Rao, Y., Single-shot COTDR using sub-chirped-pulse extraction algorithm for distributed strain sensing, *J. Lightwave Technol.*, 2020, vol. 38, no. 7, pp. 2028–2036.  
<https://doi.org/10.1364/JLT.38.002028>
- Xue, Y., Niu, Y., and Gong, S., External modulation optical coherent domain reflectometry with long measurement range, *Sensors*, 2021, vol. 21, no. 16, p. 5510.  
<https://doi.org/10.3390/s21165510>
- Yu, C., Zhan, Z., Lindsey, N.J., Ajo-Franklin, J.B., and Robertson, M., The potential of DAS in teleseismic studies: Insights from the Goldstone experiment, *Geophys. Res. Lett.*, 2019, vol. 46, no. 3, pp. 1320–1328.  
<https://doi.org/10.1029/2018GL081195>
- Yuan, Q., Chai, J., Zhang, Y., Liu, Y., and Ren, Y., Investigation of deformation pattern and movement law of the huge-thick conglomerate stratum by a large-scale 3D model test with distributed optical fiber sensor monitoring, *Sensors*, 2021, vol. 21, no. 17, p. 5985.  
<https://doi.org/10.3390/s21175985>
- Yuan, S., Lellouch, A., Clapp, R.G., and Biondi, B., Near-surface characterization using a roadside distributed acoustic sensing array, *Leading Edge*, 2020, vol. 39, no. 9, pp. 646–653.  
<https://doi.org/10.1190/tle39090646.1>
- Zhang, C.-C., Shi, B., Zhu, H.-H., Wang, B.-J., and Wei, G.-Q., Toward distributed fiber-optic sensing of sub-

- surface deformation: A theoretical quantification of ground-borehole- cable interaction, *J. Geophys. Res.: Solid Earth*, 2020, vol. 125, no. 3, p. e2019JB018878. <https://doi.org/10.1029/2019JB018878>
- Zhang, C.C., Shi, B., Zhang, S., Gu, K., Liu, S.-P., Gong, X.-L., and Wei, G.-Q., Microanchored borehole fiber optics allows strain profiling of the shallow subsurface, *Sci. Rep.*, 2021, vol. 11, p. 9173. <https://doi.org/10.1038/s41598-021-88526-8>
- Zhang, J., Zheng, H., Zhu, T., Yin, G., Liu, M., Bai, Y., Qu, D., Qiu, F., and Huang, X., Distributed fiber sparse-wideband vibration sensing by sub-Nyquist additive random sampling, *Opt. Lett.*, 2018, vol. 43, pp. 2022–2025. <https://doi.org/10.1364/OL.43.002022>
- Zhang, Y., Liu, J., Xiong, F., Zhang, X., Chen, X., Ding, Z., Zheng, Y., Wang, F., and Chen, M., A space-division multiplexing method for fading noise suppression in the  $\Phi$ -OTDR system, *Sensors*, 2021, vol. 21, no. 5, p. 1694. <https://doi.org/10.3390/s21051694>
- Zhang, Z., Fang, Z., Stefani, J., DiSiena, J., Bevc, D., Ning, I.L.C., Hughes, K., and Tan, Y., Modeling of fiber-optic strain responses to hydraulic fracturing, *Geophysics*, 2020, vol. 85, no. 6, pp. A45–A50. <https://doi.org/10.1190/geo2020-0083.1>
- Zhou, D.-P., Li, W., Chen, L., and Bao, X., Distributed temperature and strain discrimination with stimulated Brillouin scattering and Rayleigh backscatter in an optical fiber, *Sensors*, 2013, vol. 13, no. 2, pp. 1836–1845. <https://doi.org/10.3390/s130201836>
- Zhou, D.-P., Chen, L., and Bao, X., Distributed dynamic strain measurement using optical frequency-domain reflectometry, *Appl. Opt.*, 2016, vol. 55, no. 24, pp. 6735–6739. <https://doi.org/10.1364/AO.55.006735>